Coaxial Compound Helicopter for Confined Urban Operations

Wayne Johnson
Aeromechanics Office
National Aeronautics and Space Administration
Ames Research Center, Moffett Field, California

Joshua F. Elmore
Ernest B. Keen
Andrew T. Gallaher
Gerardo F. Nunez
Aviation Development Directorate – AFDD
U.S. Army Research Development, and Engineering Command
Redstone Arsenal, Alabama; Hampton, Virginia; Moffett Field, California

ABSTRACT

A rotorcraft was designed for military operations in a confined urban environment. The specifications included major increases in useful load, range, and speed relative current aircraft capabilities, with a size constraint based on the dimensions of urban streets and intersections. Analysis showed that this combination of requirements is best satisfied by a coaxial main-rotor configuration, with lift compounding to off-load the rotors at high speed, and ducted fans under the rotor disk for propulsion. The baseline design is described, and the aircraft performance is summarized for utility, attack, MEDEVAC, and cargo delivery missions. The impact on size and performance is examined for a number of excursions, including lift-offset main rotors. Technology development required to achieve this advance in capability is recommended.

INTRODUCTION[·]

Future military forces must be able to operate in a densely populated urban environment. Military operations in a megacity are complex, dangerous, and intense (Ref. 1). Urban terrain is a great equalizer for operations. The megacity multi-level structures magnify the power of the defender and diminish the attacker's advantages in firepower and mobility. Urban terrain introduces a unique challenge to aircrews and ground personnel alike with the notion of the urban canyon (Ref. 2). An urban canyon exists when an opponent is shielded by vertical structures. For the aviation community, this means air support at the street-level is needed, including at least an assault and MEDEVAC capability. The street dimensions, hence the operational constraints, vary greatly among megacities. Streets in older business sections can range from roughly 8 to 30-ft wide. More developed megacities, with design specifications for streets, may have operating dimensions closer to 60 ft. The size constraints imposed on aircraft that have to fit between buildings along these streets, and also maneuver amongst them, become a critical factor in aircraft designed for operation in the urban environment.

A rotorcraft design was developed for military operations in a confined urban environment, using the rotorcraft sizing code NDARC (NASA Design and Analysis of Rotorcraft). This aircraft is the smallest of the family of vertical lift aircraft described in Reference 3. First the paper describes the aircraft specifications, which include major increases in useful load, range, and speed relative current aircraft capabilities, with a size constraint based on the dimensions of urban streets and intersections. The paper shows that this combination of requirements can be best satisfied by a Coaxial Compound Helicopter (CCH):

[·]*Presented at the AHS Specialists' Conference on Aeromechanics Design for Vertical Lift, San Francisco, CA, January 20-22, 2016.*

a coaxial main-rotor configuration, with lift compounding to off-load the rotors at high speed, and ducted fans under the rotor disk for propulsion (Figure 1). The calibration of NDARC for the CCH performance and weights is described. A baseline aircraft that meets the specifications is presented, including the aircraft performance for utility, attack, MEDEVAC, and cargo delivery missions. The impact on size and performance is examined for a number of excursions, including lift-offset main rotors. Technology maturity and development required to achieve this advance in capability is recommended.

COMPUTATIONAL METHODS

Rotorcraft Sizing Code NDARC

NASA Design and Analysis of Rotorcraft (NDARC) is a conceptual/preliminary design and analysis computer program for rapidly sizing and conducting performance analysis of new vehicle concepts with particular emphasis on vertical lift configurations (Refs. 4–7). NDARC has a modular architecture, facilitating its extension to new concepts and the implementation of new computational procedures. NDARC version 1.8f was used in this design activity.

NDARC is an aircraft system tool that performs design and analysis tasks. The design task sizes the vehicle to satisfy a set of design conditions and missions. The analysis tasks include off-design mission analysis and flight performance calculation for point operating conditions. The aircraft size is characterized by parameters such as design gross weight, weight empty, component dimensions, drive system torque limit, fuel tank capacity, and engine power.

To achieve flexibility in configuration modeling, NDARC constructs a vehicle from a set of components, including fuselage, wings, tails, rotors, transmissions, and engines. For efficient program execution, each component uses a surrogate model for performance and weight estimation. Higher fidelity component design and analysis programs as well as databases of existing components provide the information needed to calibrate these surrogate models, including the influence of size and technology level. The reliability of the synthesis and evaluation results depends on the accuracy of the calibrated component models.

The NDARC rotor performance model represents the rotor power as the sum of induced, profile, and parasite terms: $P = P_i + P_o + P_p$. The parasite power (including climb or descent power for the aircraft) is obtained from the wind axis drag force and rotor velocity: $P_p = -XV$. The induced power is calculated from the ideal power and the induced power factor κ: $P_i = \kappa P_{\text{ideal}}$. The profile power is calculated from a mean blade drag coefficient: $C_{Po} = (\sigma/8) c_{d\,\text{mean}} F_P$, where the function F_P accounts for the increase of the blade section velocity with rotor edgewise and axial speed. The induced and profile power cannot be measured separately in a wind tunnel or flight test, only the sum is available from $P_i + P_o = P + XV$ (if the rotor wind-axis drag force X is measured or estimated). Therefore analysis is used to separate induced and profile power. In this approach, performance calculations from a comprehensive analysis are correlated with wind tunnel or flight test data; then rotor performance is calculated for the full range of expected flight and operating conditions; finally the parameters of the NDARC rotor performance model are developed based on the calculated κ and $c_{d\,\text{mean}}$.

NDARC provides default configurations and trim strategies for several common rotary wing configurations, including single main-rotor helicopters, tandem helicopters, coaxial helicopters, and tilt-rotors. In each of these default configurations, trim strategies have been defined, providing a set of starting points for a design study. Here the configuration is a coaxial rotor with fans for auxiliary propulsion. The pilot collective control commands rotor thrust, and pilot cyclic control commands lateral and longitudinal tip-path plane tilt relative the shaft (flapping). Rotor collective and cyclic pitch angles are calculated from thrust and flapping using blade element theory (Refs. 4–5).

For low speed flight, the aircraft is trimmed as usual for a helicopter: net zero force and moment on the aircraft achieved with pilot's collective stick, cyclic stick, and pedal, and aircraft pitch and roll attitude. For the coaxial configuration, collective stick is mean rotor collective and pedal is differential rotor collective. Cyclic stick goes to both rotors, with no differential cyclic control. For cruise, the aircraft is trimmed as a compound: net zero force and moment on the aircraft achieved with pilot's collective stick, cyclic stick, and pedal, fan collective, and aircraft roll attitude, for a specified aircraft pitch angle.

Comprehensive Analysis CAMRAD II

Performance analyses were conducted with the rotorcraft comprehensive analysis CAMRAD II (Ref. 8). CAMRAD II is an aeromechanics analysis of rotorcraft that incorporates a combination of advanced technologies, including multibody dynamics, nonlinear finite elements, and rotorcraft aerodynamics. The trim task finds the equilibrium solution for a steady state operating condition,

and produces the solution for performance, loads, and vibration. The flutter task linearizes the equations about the trim solution, and produces the stability results. The aerodynamic model includes a wake analysis to calculate the rotor nonuniform induced-velocities, using rigid, prescribed, or free wake geometry. CAMRAD II has undergone extensive correlation of performance and loads measurements on rotorcraft (Refs. 9–13).

The CAMRAD II aerodynamic model for the rotor blade is based on lifting-line theory, using steady two-dimensional airfoil characteristics and a vortex wake model. The rotor blade modeling problem of lifting-line theory is unsteady, compressible, viscous flow about an infinite aspect-ratio wing, in a uniform flow consisting of the yawed free stream and the wake-induced velocity. This problem is modeled as two-dimensional, steady, compressible, viscous flow (airfoil tables), plus corrections. The corrections account for swept and yawed flow, spanwise drag, and attached flow unsteady loads. Other corrections available, such as for static stall delay and dynamic stall, were not important for the operating conditions considered here. An incompressible vortex wake is behind the lifting-line, with distorted geometry and rollup. The lifting-line (bound vortex) is at the quarter chord, and the three components of wake-induced velocity are evaluated at collocation points at the three-quarter chord. This model is generally second-order accurate for section lift, which significantly improves the calculation of blade-vortex interaction loading, but less accurate for section moments. The wake analysis calculates the rotor nonuniform induced-velocity using either rigid or free wake geometry. The concentrated tip vortices are the key features of the rotor wake, important for performance, airloads, structural loads, vibration, and noise calculations. The formation of the tip vortices is modeled in CAMRAD II, not calculated from first principles.

Performance calculations for calibration of the NDARC rotor models considered first an isolated rotor, in particular to define profile power including the influence of stall. Then calculations for the coaxial rotor were used to calibrate the rotor-rotor interference effects on induced power. Rotor performance was calculated using nonuniform inflow with rigid wake geometry in high speed cruise and free wake geometry in hover. Airfoil characteristics were obtained from tables representing modern technology airfoils. For calibration of the sizing code performance, the single rotor in cruise was trimmed to a target thrust and flapping trimmed to zero, using rotor collective and cyclic at fixed shaft angle. Hover performance was calculated for a collective sweep.

AIRCRAFT SPECIFICATIONS

The design of this aircraft was driven by the need to conduct assault operations within the confines of urban streets and intersections. Review of evolving urban assault and security concepts reveals operation in urban avenues of approach of 12 to 15 m width, and re-orientation in confined spaces of 8 by 12 m (14.4 m inscribed diameter). The helicopter currently performing this role is the MELB (based on MH-6 or MD530F), which has an operating length of 32.6 ft and a width (rotor diameter) of 27.4 ft (9.9 m by 8.4 m). Thus for this investigation, the geometric constraint is 12 by 12 m (39 by 39 ft). Allowing for maneuvering space, the maximum operating dimension (width or length) was thus specified as 32 ft.

Design Mission

Figure 2 describes the design mission (urban assault), which is based on insertion/extraction of special operations or fire teams. The payload is 4 passengers of 300 lb each, for a total of 1200 lb. The mission radius is 200 km, with 30 min loiter (without payload) at midpoint. Takeoff (hover out-of-ground-effect) is at 4000 ft altitude and 95ºF (4k/95), midpoint hover is at 6000 ft and 95ºF (6k/95). The aircraft cruises at best range speed V_{br} and best altitude, for 75% of the distance (150 km). Penetration speed is at least 200 knots, at 6k/95. This mission requires significant increases in useful load, range, and speed relative current aircraft capabilities.

Small aircraft are particularly sensitive to performance requirements, so these mission specifications, although demanding, are somewhat less stringent than those anticipated for larger aircraft in a family of future military vertical lift aircraft. The vehicle resulting from these specifications can in fact lift 4 x 400 lb passengers. The system needs to be dramatically faster than existing helicopters to be responsive to the demands of the future battlefield. While achieving 230 knots would require significantly greater power, 200 knots is a reasonable compromise between weight and speed. It is assumed that the aircraft can still be transported to the operational region via existing theater assets. Increasing the radius of the design mission would just increase the fuel required and aircraft size.

The reserve fuel is the greater of 30 min or 10% of the mission fuel. Cruise and reserve segments are flown at best range speed V_{br}, which is the speed for 99% of maximum specific range (high side). Loiter is at best endurance speed V_{be}, which is the speed for minimum fuel flow. The best cruise altitude is determined by lightest

weight design, limited by onboard oxygen provisions for un-pressurized aircraft. Oxygen requirements are as follows: 10000 ft altitude and below, no oxygen needed; 10000 to 12000 ft altitude, crew must be on oxygen for durations over one hour, no passenger oxygen needed. Here the cruise mission segment is flown at 10000 ft. The penetration segment is flown at 90% MCP speed or 200 knots, whichever is higher.

Sizing Specifications

With the advanced avionics capability anticipated, the aircraft is designed for a single pilot, with no crew chief. With standard mission equipment, the aircraft is capable of being flown without a pilot (OPV). The aircraft is field-configurable as an unmanned system (UAS).

The aircraft must be foldable for rapid transportability (onload, offload, and preparation for flight), hence manual folding and a rotor brake are required. The aircraft must be transportable on the largest vehicle of the future vertical lift family, as well as on a C-17, which constrains the geometry and impacts weight.

The fuel capacity was sized to be 10% greater than the fuel for the design mission, to increase off-design flexibility. The aircraft is capable of air-to-air refueling.

The aircraft cabin is un-pressurized, while the cockpit is designed for slight over-pressure protection against nuclear-biological-chemical threats. Supplemental oxygen provisions are included.

Passenger accommodations are based on 95th percentile person, hence 23-in seat width. Cabin height is 62 in minimum, with no intrusions.

Design gross weight (DGW) is defined at the initial take-off of the sizing mission. Structural design gross weight (SDGW) is defined at the beginning of the penetration segment. Maximum takeoff gross weight (WMTO) is sized by the HOGE capability at 95% MRP and sea level, 103ºF (SL/103).

The transmission is sized by 100% MRP at SL/103, or power for 125% of 6k/95 HOGE weight. The intent of the transmission sizing specification is that the power required for 4k/95 or 6k/95 hover will be useable at SL/103 conditions. If the cruise performance requirement leads to much more installed power than needed for hover (which is the case for a number of the design excursions examined here), the transmission sizing specification is relaxed to 125% of 6k/95 HOGE power.

Equipment Weight and Drag

Table 1 defines the mission equipment weights, which were estimated using a functional build-up approach. The communications and displays weights are for the single pilot design. Navigation and pilotage weights reflect an anticipated need for Terrain Following/Terrain Avoidance (TFTA) provisions.

Table 2 defines the systems and equipment weights. The armor corresponds to modern attack rotorcraft level of protection for the pilot, and 4 lb/ft^2 cabin armor protection.

Table 3 defines weights of other useful load components. The aircraft serves as primarily an insertion/extraction platform for a four man special operations or fires team, but must have a self-defensive capability against small arms and offensive capability against light-skinned vehicles. Hence a turreted lightweight gun is installed, to reduce the demands on the pilot and to provide more rapid off-axis suppression.

The total drag increment for the equipment is $\Delta D/q = 1.38$ ft^2; composed of 0.5 ft^2 for the faired gun, 0.38 ft^2 for pilotage and targeting (faired sensor ball), and 0.5 ft^2 for aircraft survivability equipment. These drag estimates are based on effective aerodynamic fairings.

AIRCRAFT TYPES CONSIDERED

The design specifications combine a maximum operating dimension (hence maximum rotor diameters) of 32 ft, with significant load capability (1960 lb military load, 1200 lb payload, 1100 lb fuel). For these specifications, no closed solution could be found for the single main rotor and tail rotor aircraft type.

A small-wing compound with a single main-rotor was investigated (Figure 3). The configuration includes a wing, propeller, and tail rotor, similar to the AH-56 Cheyenne design. The tail rotor must be outside the main rotor disk, otherwise the moment arm is too small to provide efficient anti-torque. Hence the main rotor radius was significantly less than 32 ft, increasing the disk loading and hover power required. Sizing the tail rotor then further increased the weight and power required. The disk loading was high for both main rotor and tail rotor, hence the solidity was high, and the HOGE takeoff power was large. A converged solution (with a very large tail rotor) was only found at reduced load. The MELB demonstrates that there is a conventional helicopter solution at much reduced lift capability, range, and speed. A small-wing compound that met the geometry (32 ft) and speed (200 knots)

specifications only converged with no payload and 20% less range.

There are also solutions if the size constraint is removed. The design mission (load, speed, and range) was met with a main rotor diameter of 32 ft, hence a maximum operating dimension of 38.2 ft. The variability of the width of streets in the world's most densely populated cities could allow for the aircraft to achieve the desired operational capability by sacrificing a small percentage of accessible locations. However, such an aircraft has a design gross weight of around 11000 lb and a cruise fuel flow of 530 lb/hr, significantly larger than a corresponding coaxial design. Consequently the single main-rotor, small-wing compound configuration was not considered further in this investigation.

A tiltrotor or tiltwing might meet the specifications. Assuming a gross weight of 10000 lb, a wing with a 32-ft span and aspect ratio of 8 has a wing loading of 80 lb/ft^2. With a 4-ft wide fuselage and 1-ft clearance, the rotor diameter is 13 ft, and the disk loading of 38 lb/ft^2 implies hover power of about 3200 hp. The downwash and outwash resulting from that high disk loading would not be appropriate for operations in urban streets and intersections, therefore these aircraft types were not investigated further for this study.

An aircraft with coaxial main rotors can meet the specifications. With coaxial rotors, a tail rotor is not required for anti-torque and auxiliary propulsion can be placed under the rotor disk, hence the rotor diameter can be set to the maximum operating dimension. Other anti-torque solutions are not considered viable. For example, a rotor with tip drive has unacceptable noise and low thermal efficiency. The following sections describe the coaxial compound helicopter aircraft type.

COAXIAL COMPOUND HELICOPTER (CCH)

Figure 1 illustrates the coaxial compound helicopter (CCH) aircraft type. The configuration is compact, the main rotor disks filling the available operating dimensions (32 ft diameter). The height of the coaxial aircraft is an issue for transportability, but the aircraft will fit in the specified transport aircraft. Each rotor has a swashplate (collective and cyclic control), with torque balance provided by differential collective. Fans provide propulsion and augment yaw control. The fans are ducted for efficiency and personnel safety. The airframe, including ducted fans, fits within the footprint of the rotor disk.

The main rotors have modern hub designs with a flap frequency of 1.055/rev. The rotor performance does not rely on lift-offset. For good cruise efficiency, airframe lift is used to off-load the rotors and the fans provide all propulsive force required. Airframe lift comes from the fuselage, hubs, tail, and ducts; a canard is used to generate additional lift. The aircraft has relatively low drag, with faired hubs, retractable gear, and internal payload.

A single engine is used for simplicity and lowest cost. The hover tip speed is 725 ft/sec, the cruise tip speed is 675 ft/sec for advancing tip Mach number of 0.88 at 200 knots. This cruise rotational speed reduction of 93% can be handled by the engine with minimal loss of efficiency, so a single-speed transmission can be used.

Kamov design practices (Refs. 14-17) provide a foundation for this coaxial helicopter, in particular the selection of rotor-rotor vertical spacing (9% rotor diameter), and the rotor hub and control kinematics used to minimize blade flapping magnitude and maximize clearance. Kamov helicopters have been tested well beyond 200 knots, although their cruise speeds are substantially lower.

The computational methods NDARC and CAMRAD II were used to develop the CCH design. Both methods have been used extensively in design and aeromechanics investigations of coaxial rotorcraft (Refs. 11–13).

Aerodynamics and Performance

The rotor was sized for $C_W/\sigma = 0.095$, based on design gross weight and 4k/95 conditions. The comparable blade loading for an advanced helicopter is $C_W/\sigma = 0.09$; the larger value reflects the rotor being off-loaded in cruise.

Airframe lift comes from the fuselage, tail and ducts, hubs and fairings, and the canard. Based on analysis and test of similar configurations, the total airframe lift used is $L/q = 35$ ft^2 at cruise angle of attack, with a corresponding drag due to lift of $\Delta D/q = 2.7$ ft^2. The canard contributes about 15% of this lift. At a dynamic pressure of 100 lb/ft^2 (about 200 knots at 6k/95), the airframe lift of 3500 lb unloads the rotor by about 40%.

CAMRAD II calculations were used to calibrate the NDARC rotor performance model. Calculations for an isolated rotor defined basic induced power, and profile power including the influence of stall. Relative to a single main rotor, the coaxial rotor has less induced power at cruise, as well as rotor-rotor interference. Calculations for the coaxial rotor were used to calibrate the rotor-rotor interference effects on induced power. Figure 4 compares

the CAMRAD II and NDARC performance calculations, in terms of the rotor equivalent lift-to-drag ratio $L/D_e = LV/(P_i + P_o)$ as a function of flight speed. The rotors are operating with zero shaft angle (propulsion from the fans) and thrusts of $C_T/\sigma = 0.076$ at 100 knots and $C_T/\sigma = 0.053$ at 200 knots (airframe at constant L/q, so rotor lift decreasing with speed).

The performance model for the fans gave a propulsive efficiency of $\eta = 0.80$ to 0.82 at cruise.

The hub drag was estimated based on data for good, effective hub fairings: $(D/q)_{\text{hub}} = 0.5(W_{\text{MTO}}/2/1000)^{2/3}$.

Weights and Technology

The technology level for weight estimation was based on Army aviation S&T technology objectives, with adjustments for unique design features or approaches. Table 4 gives the technology factors used for the major weight groups. These factors were derived by first calibrating the parametric weight equations of NDARC to the closest relevant current technology aircraft (such as UH-60M, AH-64E, RAH-66, V22) or to recent aircraft designs; and then applying corrections to account for advanced technology (particularly materials) and differences in configuration or design.

Vibration reduction weight was estimated, assuming advanced technology approaches, at 1.2% of weight empty.

A contingency weight equal to 5% of weight empty was included to account for uncertainties in the parametric weight estimation methods.

Autorotation Capability

With a single engine, the rotor must be designed for adequate autorotation capability. Here the criterion was based on an autorotation index that is the ratio of the rotor kinetic energy and the hover takeoff power (Ref. 18), or $AI = KE/P = \frac{1}{2} I_{\text{rotor}} \Omega^2 / P$, where I_{rotor} is the total rotational moment of inertia of the rotor. Power and rotor rotational speed are set by other design criteria, so a specified value of the index was achieved by adding tip mass to the blade, in order to increase blade moment of inertia. The criterion used was $AI = 1.5$, which corresponds to acceptable autorotation characteristics (Ref. 18). This criterion was based on values of the index for current small helicopters: OH-6 $AI = 1.53$; MD520 $AI = 1.50$; MD600 $AI = 1.02$; and OH-58D $AI = 1.36$. This future aircraft is expected to have automatic recognition of power failure and control to maintain rotor speed, for improved autorotation characteristics.

BASELINE CCH DESIGN

Figure 5 illustrates the baseline Coaxial Compound Helicopter designed to meet the specifications of the urban assault mission. Figure 6 shows the aircraft folded, and Figure 7 shows two aircraft as transported by a C-17 or a future large vertical lift aircraft (vehicle E). Figure 8 shows details of the layout, including pilot, passengers, fuel tanks, transmission, and engine.

Design Details

Table 5 gives key design details. The design gross weight (DGW = 9416 lb) is defined at the takeoff of the sizing mission. Structural design gross weight (SDGW) is defined at the beginning of the penetration segment. The maximum takeoff gross weight (WMTO = 11672 lb) is sized by the HOGE capability at 95% MRP and SL/103. The weight empty (WE = 6702 lb) is a fixed number of the design, including pilot seat, passenger seats, and armor. The rotor weight is W_{rotor} = 759 lb. The tip weight (per blade) is required to achieve the specified autorotation index AI. The solidity is twice the single rotor value. The disk loading is based on the area of one rotor.

The takeoff power is single engine SLS IRP (2382 hp). The transmission limit is a torque limit, expressed as power at hover rotor speed. The transmission is sized by 100% MRP at SL/103. The dash speed (200 knots) is for the penetration segment weight, 95% MCP, 6k/95. The power is sized by this speed requirement; hover power gives a fallout speed of 190–195 knots. The drag increment for the equipment ($\Delta D/q = 1.38$ ft^2) increases the design gross weight by 5%, increases power by 10%. The long range cruise speed is 161 knots. Maximum speed (204 knots) is at design gross weight, 100% MCP, 6k/95.

The fuel burn is for the design mission, which has a duration of about 1.5 hr, hence reserve fuel is about 25%. The fuel tank capacity (1096 lb, 164 gallons) is sized to be 10% greater than the mission fuel. The cruise fuel flow (384 lb/hr) is a measure of efficiency. The aircraft equivalent lift-to-drag ratio is $L/D_e = WV/P$, and the aircraft figure of merit is based on gross weight and total power. The rotor equivalent lift-to-drag ratio is $L/D_e = LV/(P_i + P_o)$, and the rotor figure of merit is based on rotor thrust and rotor power.

For design excursions, aircraft purchase price increments relative this baseline design are presented. The cost was estimated using the CTM model (Ref. 19), which has an accuracy of about 20% for airframe cost.

Table 6 presents rotor, fan, lifting surface, and engine parameters of the design. The engine model is a generic advanced technology engine, scaled from a nominal size of 3000 hp. Table 7 gives the drag buildup for the basic aircraft in cruise (landing gear retracted), which is a clean design for a rotorcraft ($D/q = 1.39(W/1000)^{2/3}$). The equipment drag increment is 1.38 ft^2. Then with 2.7 ft^2 drag due to lift, the total drag is $D/q = 11.2$ ft^2.

Table 8 gives the weight empty details for the baseline CCH design.

Figure 9 compares the operating dimensions and cabin of the CCH and the MD500/530 (MELB). The CCH rotor diameter is 32 ft, while the MD500/530 rotor diameter is 27.4 ft. The length of the MD500 is 31 ft; the length of the MD530 is 32.6 ft. The disk loading is 8 lb/ft^2 for the MELB (4700 lb gross weight) and 5.25 lb/ft^2 for the MD530 (3100 lb), compared to 11.7 lb/ft^2 for the CCH.

Performance

Figure 10 shows the payload-radius for the urban assault mission. The takeoff weight at the fuel-tank corner is determined by the 6k/95 midpoint hover. The cruise segment is flown at 10000 ft. The aircraft power is sized by the 200 knot dash speed requirement. Using that power for hover gives more lift than is required for the design mission. Hence the payload capability is above the 1200 lb specification. At 200 km radius, the aircraft is capable of lifting four 400-lb passengers (1600 lb total). The fuel tank is sized 10% larger than the design mission fuel, hence the radius capability is above the 200 km required for the design mission. Also shown in Figure 10 is the lift capability (1616 lb) at the 120 nm (222 km) radius required for the Special Operations Command (SOCOM) urban assault concept of employment.

The best effort speeds as a function of altitude are shown in Figure 11, at design gross weight and ISA conditions. Here V_{MCP} is the speed using 100% MCP. The peak speed is 218 knots, at 4000-6000 ft ISA. Table 5 gives a maximum speed of 204 knots, at 100% MCP, design gross weight, and 6k/95 conditions. Table 5 also gives the dash speed of 200 knots, which is at 95% MCP, penetration weight, 6k/95.

Figure 12 shows the aircraft hover (HOGE at 100% MRP) lift capability (payload plus fuel) as a function of altitude. The aircraft gross weight is the sum of operating weight, payload, and fuel. For these calculations the operating weight is 7260 lb, which equals the empty weight (6702 lb) plus 558 lb of fixed useful load. The hot day atmosphere has a temperature of 103ºF at sea level, and 91.5ºF at 3000 ft.

The performance of the CCH is compared with that of the MD530F in Figure 13. The mission is conducted entirely at 4k/95 for the CCH (takeoff, cruise, midpoint landing) and at 5k/ISA for the MD530F. Compared to the MD530F, the CCH offers 1500 lb more lift capability, 40% more range, and 30% shorter response times.

Mission Capability

In addition to the urban assault role, the CCH is capable of performing light attack, cargo, counter-IADS, and MEDVAC missions. Table 9 lists the payload, equipment and useful load increments, and drag increments for these missions. Table 10 gives the aircraft weight at takeoff.

Light Attack Mission

Figure 14 describes the light attack mission. The payload consists of 2 JAGM, 14 rockets, and 6000 rounds 7.62 mm, for total weight of 1020 lb. The payload is expended during the midpoint loiter. The mission radius is 200 km, with 15 min HOGE and 15 min loiter at midpoint. Takeoff HOGE is at 4k/95, midpoint hover is at 6k/95. The aircraft cruises at best range speed V_{br} and best altitude (10000 ft) for 75% of the distance (150 km). Penetration speed is at least 200 knots, at 6k/95.

The CCH in light attack configuration is shown in Figure 15. The weapons are carried internally, which requires a wider door than for the urban assault mission. Figure 16 shows the payload-radius. The lift capability at 200 km radius is sufficient to carry two additional JAGM.

UAS Conversion

The aircraft is designed to be field-configurable as an unmanned system. The baseline aircraft is optionally-piloted without re-configuration. The UAS conversion removes equipment and load totaling 594 lb: pilot (250 lb), crashworthy/ armored pilot seat (160.4 lb), cockpit controls (20 lb), cabin armor (68.4 lb), passenger seats (80 lb), and survival kit (15 lb). The desired ranges require more fuel than in the standard tanks (1096 lb), so a 788 lb (118 gal, 15.7 ft^3) auxiliary fuel tank is added in the cockpit. The UAS kit adds 137 lb: additional electronics (50 lb), and the auxiliary fuel tank (86.7 lb).

Cargo UAS Mission

Figure 17 describes the cargo UAS mission. The payload is 1200 lb, carried in the cabin. The payload is dropped at the midpoint. The mission radius is 424 km, with 5 min loiter at midpoint. Takeoff HOGE is at SL/103, midpoint

hover is at 6k/95. The aircraft cruises at best range speed V_{br} and best altitude (10000 ft) for the entire radius.

The CCH in cargo UAS configuration is shown in Figure 18. Figure 19 shows the payload-radius. The performance of the CCH cargo UAS is compared with that of the KMAX in Figure 20, for missions conducted entirely at 4k/95 (takeoff, cruise, midpoint landing). For CCH performance with external load, 50 ft^2 additional drag was assumed. Payloads up to 2500 lb covered 65% of KMAX deliveries during operations in Afghanistan. At that payload, the CCH offers significantly greater radius capability.

Counter-IADS UAS Mission

Figure 21 describes the counter-IADS (Integrated Air Defense System) mission. The payload is two AGM-88E HARMs (1600 lb). The mission radius is 424 km, with the payload expended at midpoint. Takeoff HOGE is at SL/103. The aircraft cruises at best range speed V_{br} and best altitude (10000 ft) for 75% of the distance (318 km). Penetration speed is at least 200 knots, at 6k/95.

Figure 22 shows the CCH counter-IADS UAS configuration. The HARMs are carried externally, which increases the drag by 6 ft^2. Figure 23 shows the payload-radius.

MEDEVAC Mission

Figure 24 describes the MEDEVAC mission. The payload consists of a critical care team (500 lb), litter (25 lb), and medical kits (100 lb) for a total of 625 lb on the ingress segment; plus one 335-lb patient returning for a total of 960 lb. The mission radius is 200 km, with 10 min loiter at midpoint. Takeoff HOGE is at 4k/95, midpoint hover is at 6k/95. The aircraft cruises at maximum continuous power speed and best altitude (10000 ft) for the entire radius.

Figure 25 shows the MEDEVAC configuration. The payload-radius is shown in Figure 26. The aircraft is capable of a 230 km radius.

Deployment

The CCH can be carried in a mission-ready configuration by a large transport aircraft, or the CCH can self-deploy in a UAS configuration. The desired capability is 2100 nm range with headwinds, 10% fuel reserve, and takeoff and landing at SL/103. With a single engine and long duration (about 17 hours), this mission is best done without a pilot. In order to account for the self-deploy capability, the drive limit was increased to 2350 hp (for more lift) and the fuselage weight increased by 100 lb (for external tank installation and structure); the result was an increase in weight empty by 215 lb. The aircraft was flown in OPV configuration, without the pilot, gun, ammunition, and passenger seats. For the 2100 nm mission (zero payload), the (rolling) takeoff weight is 18200 lb, which is 1.9 times the structural design gross weight. The takeoff fuel required is 9976 lb, using a 3000-lb cabin auxiliary tank and a 5831-lb external auxiliary tank (drag increment 1.8 ft^2). The block time is 17 hours, and the block speed is 124 knots. Figure 27 shows the zero-wind payload-range for this configuration.

For rapid operational deployment, a more practical configuration is the piloted aircraft with a 3000-lb internal cabin auxiliary fuel tank. The aircraft is configured as mission-ready, only requiring removal of the cabin auxiliary tank. Figures 28 and 29 show the payload-range and response time, flying at best range speed and maximum speed, respectively. Takeoff is at maximum HOGE weight, SL/103. Cruise is at 6000 to 10000 ft. With only standard fuel tanks, the zero-payload range is 300–340 nm. With the auxiliary fuel tank, flying at best range speed, the zero-payload range is over 1400 nm, with a block speed of 166 knots. For maximum speed (100% MCP), the zero-payload range is almost 1300 nm, with a block speed of 192 knots.

DESIGN EXCURSIONS

A number of design excursions were examined, to identify the impact of specification changes and to explore the robustness of the CCH configuration to design changes. Key aircraft size and performance parameters are compared to the baseline design, following the format of Table 5.

Twin Engines

Table 11 shows the impact of designing the aircraft with twin engines. With two engines, the rotor moment of inertia is determined by the blade inertia; adding weight in order to meet the autorotation requirement is not necessary. However the two engines are individually less efficient than a single engine. The resulting twin engine design is about the same size as the single engine design. Historical data for airframe cost shows a significant reduction for single engine, compared to multiple engines. The CTM cost model (Ref. 19) has a factor of 0.736 for single engine, relative to multi-engine, probably reflecting general aircraft complexity as well as simply the number of engines. The cost of a twin-engine design is estimated at 8–10% greater than that of a single-engine design.

Hence the cost increase of the twin-engine design is about $1.1M.

Also shown in Table 11 is the result if the autorotation requirement is not used. Meeting the autorotation index (AI) specification requires 13.0 lb per blade, a total of 104 lb tip weight, increasing the weight empty by almost 300 lb.

ITEP Engine

The Improved Turbine Engine Program (ITEP) is developing the technology for a 3000 hp-class engine (Ref. 20), which is the right size for this CCH aircraft. Table 12 compares the baseline CCH design obtained using the generic engine model, with the design obtained using an ITEP engine model, scaled to the required power (2528 hp). Table 13 compares the generic and ITEP engine models used. The two models have different rating structure (ITEP MRP is less), specific power (ITEP mass flow is more), and specific fuel consumption (ITEP is less). The two models have about the same specific weight and lapse rate (4k and 6k power relative to sea level power). Consequently the baseline and ITEP scaled designs in Table 12 are similar.

The ITEP fixed design (Table 12) uses all 3000 hp of the nominal ITEP engine model. The fan thrust is sized for maximum speed (100% MCP), which increases to 216 knots. Since that is much more power than is needed to hover, the maximum takeoff weight was set to 125% design gross weight, and the transmission was sized at 130% design gross weight. The resulting aircraft is significantly larger than the baseline.

The ITEP derated design (Table 12) uses the 3000 hp engine, but with the transmission limit fixed at 2150 hp and the fan thrust not sized for maximum speed. The resulting aircraft is closer to the size of the design using a scaled engine.

Two Pilots

Table 14 compares the baseline aircraft with the aircraft designed to operate with two pilots. With two pilots the fixed weights are increased by 226 lb (seat 70 lb, flight controls 42.5 lb, armor 47.4+66 lb), and the second pilot weight is 250 lb. The CCH design is robust: a closed solution is obtained. The increased requirement results in a larger aircraft.

A smaller aircraft is obtained by designing for two-pilot capability: the aircraft has the fixed weights for two pilots, but the design mission was flown with just one pilot.

Rotor Diameter, Mission Range, and Dash Speed

Table 15 shows the designs for a number of excursions. With a 40-ft rotor diameter (instead of 32 ft), the principal change is a significant reduction in disk loading, hence reduction in downwash/outwash. With this larger rotor, the hover efficiency (lb/hp) improves, so the cruise power is much more than is needed to hover (hover power is 67% MRP, instead of 83% MRP for the baseline design). Hence the maximum takeoff weight was set to 125% design gross weight, and the transmission was sized at 130% design gross weight. Also, the number of blades per rotor was reduced to three, so the blade aspect ratio is not too high.

Another excursion involved designing for a 370 km mission radius (200 nm instead of 200 km). Again, the CCH design is robust. The increased specification results in a larger aircraft, primarily due to the greater fuel burn.

Table 15 also shows the aircraft designed for 230 knots dash speed. The cruise power is much more than is needed to hover, so the maximum takeoff weight was set to 125% design gross weight, and the transmission was sized at 130% design gross weight. The result is a much larger aircraft: design gross weight increased 14%, installed power increased 51%. The impact of this weight and power increase is a significant aircraft cost increase (based on Ref. 19).

Six Passengers

Table 16 shows the impact of increasing the number of passengers to six. Figure 30 shows the configuration. The fuselage to accommodate six passengers is 24 in wider than the baseline, which increases the fuselage wetted area to 525 ft^2 (from 400 ft^2 for four passengers). The result was an increase in the airframe drag of 0.77 ft^2. The wider fuselage was 96 lb heavier. The cabin equipment was increased by 86 lb (seats 40 lb, OBIGGS/OBOGS 10 lb, cabin armor 36 lb). The result is a much larger aircraft.

A smaller aircraft is obtained (Table 16) by designing for six-passenger capability: the fuselage and power are sized for the six passengers, but the design mission is flown with only four passengers.

Disk Loading and Rotor Diameter

Table 17 shows the impact of reducing the disk loading, by relaxing the rotor diameter constraint. With a larger diameter the cruise power is much more than is needed to hover, so the maximum takeoff weight was set to 125% design gross weight, and the transmission was sized at

130% design gross weight. Also, the number of blades per rotor was reduced to three.

With a 39.5-ft diameter rotor, the disk loading matches that of the UH-60 Blackhawk: UH-60M maximum takeoff weight (internal load) of 22000 lb gives a disk loading of 9.73 lb/ft^2.

Table 18 shows a disk loading sweep for an aircraft design using the ITEP engine (derated, transmission limit 2150 hp and fan thrust sized for 200 knots), with capability for two pilots and six passengers (design mission flown with one pilot and four passengers). Flying the design mission with two pilots and six passengers resulted in a vehicle weight of about 11700 lb. With a 41.5 ft diameter rotor, the disk loading matches that of the UH-60 Blackhawk.

Figure 31 summarizes the variation of the design gross weight with rotor diameter for the baseline configuration, and for the aircraft with ITEP engine, two pilots, and six passengers. Lines of constant disk loading are shown; based on design gross weight, the UH-60 disk loading is 7.8 lb/ft^2. The design gross weight does not vary much with disk loading because the installed power was sized by the cruise conditions, and because the maximum takeoff weight and transmission limit were based on the installed power only for the 32-ft diameter designs.

Since the aircraft power was determined by the cruise condition, the principal impact of disk loading is on the outwash characteristics. The Paxman force (Ref. 21) is a measure of the action of the rotorcraft outwash on a person, which depends on the height and shape of the outwash velocity field, as well on the velocity magnitude (which follows from the disk loading). Figure 31 shows a line for constant Paxman force, equivalent to the UH-60 value. Since the CCH aircraft is smaller than the UH-60, the CCH produces the same force at higher disk loading. The baseline design at 32-ft diameter produces less force than a UH-60, even though the disk loading is almost 12 lb/ft^2. The larger aircraft (ITEP engine, two pilots, six passengers) produces that same force as from a UH-60 at 34.5-ft diameter. Thus with a criterion based on personnel operating in the outwash field, the higher disk loading of the aircraft constrained by the urban operations should be acceptable.

If the size constraint based on the dimensions of urban streets and intersections is eliminated entirely, then other rotorcraft configurations become viable candidates, notably a small-wing compound helicopter with a single main rotor.

LIFT OFFSET ROTORS

A lift-offset rotor is a hingeless rotor that can attain good efficiency at high speed, by operating with more lift on the advancing side than on the retreating side of the rotor disk (Refs. 11–12). By operating a rotor in edgewise flight with lift offset, attaining good performance at high forward speed is possible. A conventional rotor with an articulated hub is constrained to operate with small hub moments. In forward flight, the retreating side of the disk is not able to generate much lift because of low dynamic pressure and stall, so for roll moment balance the advancing side is not allowed to generate much lift either. The resulting load distribution over the rotor disk is far from optimum for either induced or profile power losses, and the rotor efficiency and lift capability steadily decrease with forward speed. Even hingeless and bearingless rotors are generally not designed for the blades and hubs to carry significant roll moment, and thus encounter similar aerodynamic performance limitations. However, a very stiff hingeless rotor can be designed that will permit operation with significant roll moment, typically with rotor lift offsets of 20%. Roll moment balance of the entire aircraft requires either twin main rotors or perhaps a wing. The lift offset concept was demonstrated for the coaxial configuration (Advancing Blade Concept) by the XH-59A flight demonstration program of the 1970s (Ref. 22). While confirming the basic viability of the concept, the aerodynamic performance of the XH-59A was compromised by the choice of airfoils, planform, and twist, as well as by high hub drag. In addition, the stiff hingeless rotors led to a heavy hub design and high vibration in flight. Recently the capability of lift-offset rotors has been re-examined, including the impact of current and advanced technology (Refs. 23–24).

By carrying a significant roll moment, the rotor profile power and induced power can be greatly reduced in high speed edgewise flight. CAMRAD II calculations were used to calibrate the NDARC rotor performance model. Figure 32 compares the CAMRAD II and NDARC performance calculations, in terms of rotor equivalent lift-to-drag ratio as a function of flight speed. The rotors are operating with zero shaft angle and a lift offset of 0.25R.

Taking advantage of the better lift capability, the lift-offset rotor was sized for $C_W/\sigma = 0.116$, based on design gross weight and 4k/95 conditions. Considering the larger frontal area of the hingeless rotors, the hub drag was estimated using $(D/q)_{\text{hub}} = 0.597(W_{\text{MTO}}/2/1000)^{2/3}$. Vibration reduction weight was estimated at 2.6% of weight empty.

Table 19 compares the baseline CCH and lift-offset compound (LOC) designs. The lift-offset rotor has better performance from less blade area. Primarily because of the higher rotor weight (needed to carry the hub roll moments), the aircraft weight empty, power, fuel burn, and cost are higher for the LOC. These results are consistent with lift-offset designs for other missions and larger aircraft.

RECOMMENDED TECHNOLOGY MATURATION

The Coaxial Compound Helicopter designs presented here are based on estimates of component weights and performance. The performance can be verified first by wind tunnel tests and then by flight tests of the configuration. Such tests would also provide substantiation of the structural loads, from which detailed designs can be made to confirm the weights.

The impact of aerodynamic interference on the aircraft handling qualities, loads, and performance must be established through test and calculations, and design solutions found for any problems encountered. While that statement is true of any rotorcraft, the CCH configuration with coaxial rotors, canard and tail plane, fans and ducts has more possibilities for interference issues. Exploring and solving the interactional aerodynamic phenomena of the CCH before (instead of during) the flight test is recommended.

Taking the coaxial configuration to high speed may be expected to introduce interesting dynamics phenomena. The blade tip clearance must be maintained in all conditions, particularly in high speed or high load maneuvers. Tip-path-plane control should be developed (including flight test), using sensing of the blade flap motion, fed back to blade pitch control, either in the rotating or non-rotating frame.

With a single engine, the rotor must be designed for adequate autorotation capability. Specifically, acceptable autorotation characteristics are achieved by adding tip weights in order to increase the rotor rotational inertia. For improved autorotation characteristics, automatic recognition of power failure and control to maintain rotor speed should be developed for this aircraft. Perhaps the improvements achieved with control will permit reduced rotor weight.

SUMMARY AND CONCLUSIONS

NDARC was used to define a rotorcraft design for military operations in a confined urban environment. Table 20 summarizes the baseline specifications and resulting fallout capability. The specifications included major increases in useful load, range, and speed compared to current aircraft capabilities, with a 32-ft operating size constraint based on the dimensions of urban streets and intersections. Analysis showed that this combination of specifications is best satisfied by a coaxial main-rotor configuration, with lift compounding to off-load the rotors at high speed, and ducted fans under the rotor disk for propulsion.

The baseline specifications are met by a Coaxial Compound Helicopter (CCH) with a design gross weight of 9400 lb and installed takeoff power of 2400 hp. The aircraft power is sized by the 200 knot dash speed specification. Using that power for hover gives more lift than is required for the design mission. Hence the payload capability is above the 1200 lb specification. At 200 km radius, the aircraft is capable of lifting four 400 lb passengers (1600 lb total). The fuel tank is sized 10% larger than the design mission fuel, hence the radius capability is above the 200 km required for the design mission.

The baseline CCH design is robust, so while increasing a requirement resulted in a larger aircraft, a closed design solution was still obtained. Table 20 summarizes the results of several design excursions, in terms of weight and power increases. Extending the mission radius to 370 km increased the weight by 700 lb. Accommodating six passengers added up to 1400 lb and 375 hp. Two-pilot operation increased the weight by up to 700 lb. Increasing the design speed to 230 knots added 1335 lb and 1200 hp. Using a derated ITEP engine added at least 250 lb, but a new engine development program would not then be required. A twin-engine design added about 200 lb, and at least $1M in purchase cost. An aircraft could be designed with even greater capability than these examples, at the cost of additional weight and power.

The baseline specifications represent a good balance of capability. The CCH meets these specifications at a practical weight and power, with good operational suitability. The technology maturation and development needed to achieve this capability includes work on interactional aerodynamics of the configuration and the dynamics of high-speed coaxial rotors.

REFERENCES

1) United States Army. “The Megacity: Operational Challenges For Force 2025 And Beyond.” Army Capabilities Integration Center, Report HD-228176, August 2014.

2) United States Army. “The Infantry Battalion.” Field Manual 3-21.20, December 2006.

3) Keen, E.B., and Tenney, B.S. “Keen, E.B., and Tenney, B.S.” AHS Specialists’ Conference on Aeromechanics Design for Vertical Lift, San Francisco, CA, January 2016.

4) Johnson, W. “NDARC. NASA Design and Analysis of Rotorcraft.” NASA TP 2015-218751, April 2015.

5) Johnson, W. “NDARC — NASA Design and Analysis of Rotorcraft. Theoretical Basis and Architecture.” American Helicopter Society Specialists’ Conference on Aeromechanics, San Francisco, CA, January 2010.

6) Johnson, W. “NDARC — NASA Design and Analysis of Rotorcraft. Validation and Demonstration.” American Helicopter Society Specialists’ Conference on Aeromechanics, San Francisco, CA, January 2010.

7) Johnson, W. “Propulsion System Models for Rotorcraft Conceptual Design.” Fifth Decennial AHS Aeromechanics Specialists’ Conference, San Francisco, CA, January 22-24, 2014.

8) Johnson, W., “Technology Drivers in the Development of CAMRAD II,” American Helicopter Society Aeromechanics Specialist Meeting, San Francisco, California, January 1994.

9) Johnson, W. “Rotorcraft Aeromechanics Applications of a Comprehensive Analysis.” HeliJapan 1998: AHS International Meeting on Rotorcraft Technology and Disaster Relief, Gifu, Japan, April 1998.

10) Yeo, H., Bousman, W. G., and Johnson, W., “Performance Analysis of a Utility Helicopter with Standard and Advanced Rotor,” *Journal of the American Helicopter Society*, Vol. 49, No. 3 (July 2004).

11) Johnson, W. “Influence of Lift Offset on Rotorcraft Performance.” NASA TP 2009-215404, November 2009.

12) Johnson, W.; Moodie, A.M.; and Yeo, H. “Design and Performance of Lift-Offset Rotorcraft for Short-Haul Missions.” American Helicopter Society Future Vertical Lift Aircraft Design Conference, San Francisco, CA, January 2012.

13) Yeo, H., and Johnson, W. “Prediction of Maximum Lift Capability of Helicopter Rotors.” *Journal of Aircraft*, Vol. 52, No. 1, (January-February 2015).

14) Kasjanikov, V.A. “Coaxial Helicopters — Current Status and Future Developments.” *Vertiflite*, Vol. 36, No. 5 (September/October 1990).

15) Bourtsev, B.N., and Selemenev, S.V. “Blade Flap Motion and Lower-to-Upper Rotor Blade Tips Clearances of Coaxial Helicopters.” Journal of the *American Helicopter Society*, Vol. 41, No. 1 (January 1996).

16) Bourtsev, B.N.; Selemenev, S.V.; and Vagis, V.P. “Coaxial Helicopter Rotor Design and Aeromechanics.” Twenty-Fifth European Rotorcraft Forum, Rome, Italy, September 1999.

17) Mikheyev, S.V.; Bourtsev, B.N.; Danilkina, V.L.; Ivannikova, R.V.; Selemenev, S.V.; and Schetinin, Y.S. “Kamov Composite Blades.” Thirty-First European Rotorcraft Forum, Florence, Italy, September 2005.

18) Wood, T.L. “High Energy Rotor System.” American Helicopter Society 32nd Annual National V/STOL Forum, Washington, D.C., May 1976.

19) Harris, F.D., and Scully, M.P. “Rotorcraft Cost Too Much.” Journal of the American Helicopter Society, Vol. 43, No. 1, January 1998.

20) United States Army. "Army Equipment Program in Support of President's Budget 2016." Office of the Deputy Chief of Staff, G-8 Future Force Division, April 2015.

21) Silva, M.J., and Riser, R. “CH-47D Tandem Rotor Outwash Survey.” American Helicopter Society 67th Annual Forum, Virginia Beach, VA, May 2011.

22) Ruddell, A.J., and Macrino, J.A. “Advancing Blade Concept (ABC) High Speed Development.” American Helicopter Society 36th Annual Forum, Washington, D.C., May 1980.

23) Bagai, A. “Aerodynamic Design of the X2 Technology Demonstrator™.” American Helicopter Society 64th Annual Forum, Montreal, Canada, April 2008.

24) Walsh, D.; Weiner, S.; Arifian, K.; Lawrence, T.; Wilson, M.; Millott, W.; and Blackwell, R. “High Airspeed Testing of the Sikorsky X2 Technology™ Demonstrator.” American Helicopter Society 67th Annual Forum, Virginia Beach, VA, May 2011.

NOMENCLATURE

Acronyms and Subscripts

CAMRADII	Comprehensive Analytical Model of Rotorcraft Aerodynamics and Dynamics
CCH	Coaxial Compound Helicopter
DGW	design gross weight
HOGE	hover out of ground effect
IADS	Integrated Air Defense Systems

IRP	intermediate rated power
ISA	International Standard Atmosphere
ITEP	Improved Turbine Engine Program
LOC	lift-offset compound
MEDEVAC	medical evacuation
MELB	mission-enhanced little bird
MCP	maximum continuous power
MRP	maximum rated power
NDARC	NASA Design and Analysis of Rotorcraft
OPV	optionally-piloted vehicle
sfc	specific fuel consumption
SDGW	structural design gross weight
SLS	sea level standard
UAS	unmanned aerial system
WE	weight empty
WMTO	maximum takeoff weight

Symbols

A	rotor disk area, πR^2
AI	autorotation index
$c_{d\ \mathrm{mean}}$	mean drag, $C_{Po} = (\sigma/8)c_{d\ \mathrm{mean}}F_P$
C_{Po}	profile power coefficient, $P_o/\rho A V_{\mathrm{tip}}^3$
C_W	weight coefficient, $W/\rho A V_{\mathrm{tip}}^2$
C_T	rotor thrust coefficient, $T/\rho A V_{\mathrm{tip}}^2$
D	drag
F_P	profile power speed factor
FM	hover figure of merit
I_{rotor}	rotor rotational inertia
L	lift; rotor wind-axis lift
L/D_e	equivalent lift-to-drag ratio, $LV/(P_i + P_o)$ for rotor, WV/P for aircraft
P	rotor power
P_i	rotor induced power
P_{ideal}	rotor ideal induced power
P_o	rotor profile power
P_p	rotor parasite power, $-XV$
q	dynamic pressure, $\frac{1}{2}\rho V^2$
Q	drive train torque
R	rotor blade radius
T	rotor thrust
V	flight speed
V_{br}	best range speed (99% high side)
V_{be}	best endurance speed
V_{MCP}	max continuous power speed
V_{tip}	rotor tip speed, ΩR
W	weight
X	rotor wind-axis drag
κ	induced power factor, $P_i = \kappa P_{\mathrm{ideal}}$
ρ	air density
Ω	rotor rotational speed

Operating Condition

4k/95	4000 ft altitude, 95ºF
6k/95	6000 ft altitude, 95ºF
10k/ISA	10000 ft altitude, standard temperature
SL/103	sea level, 103ºF

Table 1. Mission equipment weights (lb).

Avionics Group (mission equipment)	660	
communications		123
navigation / pilotage		234
processing		116
displays		62
aircraft survivability equipment		95
racks / supports		30

Table 2. Systems and Equipment Weights (lb).

Electrical Group	380	
generator/alternator		80
battery		30
power conversion		30
power distribution		160
lights / blade tracking		60
supports		20
Armament group — Armor	211.8	
pilot seat		47.4
additional cockpit		66.0
wire strike		15.0
engine armor		15.0
cabin floor armor		68.4
Furnishings and Equipment Group	288	
crew seat		70
troop seats (4x20)		80
acoustic / thermal insulation		54
emergency equipment		24
miscellaneous equipment		40
OBIGGS / OBOGS		20
Environmental Control Group	84	
Load and Handling Group	26	
aircraft handling		8
internal cargo		18

Table 3. Other Useful Load Weights (lb).

crew	250
trapped fluids	23
survival kits	15
turret installation	150
M240 gun	50
ammunition (500 rounds 7.62mm)	40
chaff/flare	30

Table 4. Principal technology factors.

main rotor blade	0.861
main rotor hub	0.827
fan	0.577
fuselage	0.861
landing gear	0.917
fuel tank	0.722
rotor flight controls	0.712

Table 5. Key design details of baseline CCH.

DGW	lb	9416
WMTO	lb	11672
WE	lb	6702
W_{rotor}	lb	759
AI	sec	1.50
tip weight	lb	13.0
solidity		2x0.061
disk loading	lb/ft^2	11.7
P takeoff	hp	2382
Q limit	hp	2100
V dash	knots	200
V max	knots	204
fuel burn	lb	812
fuel tank	lb	1096
cruise fuel flow	lb/hr	384
aircraft L/D_e		5.3
aircraft FM		0.63
rotor L/D_e		10.6
rotor FM		0.76

Table 6. Aircraft design parameters.

Rotors		main rotor	fan
disk loading	lb/ft^2	11.7	80.0
design C_W/σ (at 4k/95)		0.095	0.145
radius	ft	16	1.62
solidity (thrust-weighted)		0.061	0.450
chord (thrust-weighted)	ft	0.767	0.327
blade aspect ratio		20.8	5.0
number of blades		4	7
rotation direction		lower CW	right CCW
hover tip speed	ft/sec	725	800
cruise tip speed	ft/sec	675	745
autorotation index		1.5	
blade tip weight	lb	13.0	
rotor incidence	deg	–4	0
Lifting Surfaces		canard	horizontal tail
area	ft^2	26.9	33.6
span	ft	11.2	14.1
chord	ft	2.4	2.4
aspect ratio		4.65	5.9
rotor-rotor separation	fraction diameter	0.09	
fuselage length	ft	27.5	
fuselage width	ft	4.5	
fuselage height	ft	6	
airframe wetted area	ft^2	579	
fuel tank capacity	lb	1096	
drive system limit	hp	2100	
number of engines		1	
takeoff power (IRP)		2382	
SLS power MCP	hp	2010	
SLS power MRP	hp	2550	
MCP SLS sfc	lb/hp-hr	0.385	
MCP SLS fuel flow	lb/hr	774	
MCP SLS gross jet thrust	lb	108	
engine weight	lb	381	
weight / power	lb/hp	0.160	

Table 7. Cruise drag buildup, D/q (ft^2).

aircraft	7.15	
fuselage		1.64
fittings and fixtures		0.40
rotor-body interference		0.30
main rotor hubs		3.24
fan hubs		0.13
ducts		0.95
canard		0.22
tail		0.27

Table 8. Weight statement for baseline CCH design.

	lb	tech factor
WEIGHT EMPTY	6702.2	
STRUCTURE	2259.5	
wing group (canard)	56.5	
rotor group	759.1	
blade assembly	538.0	0.861
hub & hinge	221.1	
basic	209.0	0.827
blade fold	12.0	0.850
empennage group (hor tail)	76.7	
basic	54.7	0.667
fold	22.0	
fuselage group	957.5	
basic	902.6	0.800
marinization	7.9	
pressurization	7.9	0.880
crashworthiness	39.0	0.850
alighting gear group	369.1	
engine section or nacelle group	21.9	1.104
air induction group	18.6	1.104
PROPULSION GROUP	1659.4	
engine system	555.1	
engine	380.6	
exhaust system	106.6	
accessories	68.0	1.005
prop/fan installation	98.4	0.577
hub & hinge	35.0	
rotor/fan duct	63.4	
fuel system	279.4	
tanks and support	122.2	0.722
plumbing	157.2	0.721
drive system	726.4	
gear boxes	590.2	0.738
transmission drive	23.3	0.690
rotor shaft	88.2	0.738
rotor brake	24.6	

	lb	tech factor
SYSTEMS AND EQUIPMENT	2367.8	
flight controls group	495.6	
cockpit controls	42.5	fixed
automatic flight control system	110.0	fixed
system controls	343.1	
fixed wing systems	17.2	
non-boosted	10.2	0.501
boost mechanisms	6.9	0.702
rotary wing systems	325.9	
non-boosted	106.2	0.646
boost mechanisms	187.8	0.712
boosted	31.9	0.459
instruments group	50.0	fixed
hydraulic group	64.0	0.712
electrical group	399.0	
aircraft	380.0	fixed
anti-icing	19.0	
avionics group (mission equip)	660.0	fixed
armament group (armor)	211.8	fixed
furnishings & equipment group	288.0	
environmental control group	84.0	fixed
anti-icing group	89.5	
load & handling group	26.0	fixed
VIBRATION	80.4	
CONTINGENCY	335.1	
DESIGN GROSS WEIGHT	9416.4	
Structural Design GW	9181.4	
Weight Maximum Takeoff	11672.5	

Table 9. Mission payload, equipment and useful load increments, and drag increment.

Mission		Urban Assault	Cargo UAS	Counter-IADS UAS	MEDEVAC	Light Attack
payload, internal	lb	1200 (a)	1200		960	1020 (f)
payload, external	lb			1600 (b)		
equipment and useful load						
turret installation	lb	150 (c)	150 (c)	150 (c)	150 (c)	150 (d)
gun	lb	50 (c)		50 (c)		50.7 (d)
ammunition	lb	40 (e)		40 (e)		
weapons installation	lb					236.8
launchers	lb			135		142
targeting / DVE / TFTA	lb					150
survival kits	lb	15			15	15
chaff/flare	lb	30	30	30	30	30
forward auxiliary fuel tank	lb		86.7	86.7		
additional electronics	lb		50	50		
litter mounts	lb				25	
hoist provisions	lb				40	
hoist	lb				100	
number of crew seats		1	0	0	1	1
number of passenger seats		4	0	0	2	0
pilot seat	lb	70			70	70
passenger seats	lb	80			40	0
cockpit controls	lb	47.5	27.5	27.5	47.5	47.5
cabin armor	lb	68.4	0	0	68.4	0
crew armor	lb	47.4	0	0	47.4	47.4
cockpit armor	lb	66	23	23	66	66
drag increment						
faired gun	ft^2	0.5	0.5	0.5	0.5	0.5
AGM-88E HARM	ft^2			6.0 (c)		
pilotage and targeting (faired sensor ball)	ft^2	0.38	0.38	0.38	0.38	0.77
aircraft survivability equipment	ft^2	0.5	0.5	0.5	0.5	0.5
total D/q	ft^2	1.38	1.38	7.38	1.38	1.77

(a) 4 passengers; (b) 2 AGM-88E HARMs; (c) M240 gun; (d) M134 Minigun; (e) 500 rounds 7.62mm; (f) including ammunition

Table 10. Aircraft weight at mission start (takeoff).

Mission		Urban Assault	Cargo UAS	Counter-IADS UAS	MEDEVAC	Light Attack
gross weight	lb	9473.9	9264.9	9918.3	8799.2	9700.9
payload	lb	1200.0	1200.0	1600.0	625.0	1020.0
number of passengers		4	0	0	0	0
fuel weight	lb	1013.6	1351.8	1380.2	878.9	1079.6
fuel burned	lb	811.8	1164.2	1190.4	678.3	885.3
reserve fuel	lb	201.9	187.5	189.4	200.3	194.3
operating weight	lb	7260.2	6713.1	6938.1	7295.2	7601.3
weight empty	lb	6702.2	6702.2	6702.2	6702.2	6702.2
fixed useful load	lb	558.0	10.9	235.9	593.0	899.1
number of crew		1	0	0	1	1
crew	lb	250	0	0	250	250
fluids	lb	23	23	23	23	23
auxillary fuel tanks	lb	0	86.68	86.68	0	0
other fixed useful load	lb	285	180	405	195	245.7
gross weight	lb	9473.9	9264.9	9918.3	8799.2	9700.9
weight empty	lb	6702.2	6702.2	6702.2	6702.2	6702.2
useful load	lb	2771.6	2562.7	3216.1	2096.9	2998.7
fixed useful load	lb	558.0	10.9	235.9	593.0	899.1
payload	lb	1200.0	1200.0	1600.0	625.0	1020.0
fuel weight	lb	1013.6	1351.8	1380.2	878.9	1079.6

Table 11. Twin engine design excursion.

		Baseline	no AI	twin engine
number engines		1	1	2
DGW	lb	9416	9115	9577
WMTO	lb	11692	11578	11910
WE	lb	6702	6420	6789
W_{rotor}	lb	759	538	557
AI	sec	1.50	0.73	0.72
tip weight	lb	13.0	0.0	0.0
solidity		2x0.061	2x0.059	2x0.062
disk loading	lb/ft^2	11.7	11.3	11.9
P takeoff	hp	2382	2365	2483
Q limit	hp	2100	2084	2189
V dash	knots	200	200	200
V max	knots	204	204	204
fuel burn	lb	812	797	876
fuel tank	lb	1096	1076	1184
cruise fuel flow	lb/hr	384	371	412
aircraft L/D_e		5.3	5.3	5.2
aircraft FM		0.63	0.62	0.62
rotor L/D_e		10.6	10.8	10.5
rotor FM		0.76	0.76	0.76
cost increment	$M	—	–0.2	~+1.1

Table 12. ITEP engine design excursion.

		Baseline	ITEP scaled	ITEP derated	ITEP fixed
DGW	lb	9416	9456	9661	9979
WMTO	lb	11692	11805	12076	12474
WE	lb	6702	6777	6915	7209
W_{rotor}	lb	759	785	786	880
AI	sec	1.50	1.50	1.50	1.50
tip weight	lb	13.0	14.6	14.1	19.1
solidity		2x0.061	2x0.061	2x0.063	2x0.065
disk loading	lb/ft^2	11.7	11.8	12.0	12.4
P takeoff	hp	2382	2528	3000	3000
Q limit	hp	2100	2145	2150	2545
V dash	knots	200	200	200	200
V max	knots	204	204	204	216
fuel burn	lb	812	778	835	853
fuel tank	lb	1096	1051	1127	1152
cruise fuel flow	lb/hr	384	372	405	419
aircraft L/D_e		5.3	5.1	5.0	5.0
aircraft FM		0.63	0.63	0.63	0.63
rotor L/D_e		10.6	10.6	10.5	10.3
rotor FM		0.76	0.76	0.76	0.76
cost increment	$M	—	+0.2	+0.8	+1.0

Table 13. Key parameters for generic engine model and ITEP engine model.

		generic 3000 hp	generic scaled	ITEP 3000 hp	ITEP scaled
SLS power MCP	hp	2532	2010	2550	2149
SLS power IRP	hp	3000	2382	3000	2528
SLS power MRP	hp	3212	2550	3076	2592
SLS power CRP	hp	3366	2673	3136	2642
MCP/IRP		0.844	0.844	0.850	0.850
IRP/IRP		1.000	1.000	1.000	1.000
MRP/IRP		1.071	1.071	1.025	1.025
CRP/IRP		1.122	1.122	1.045	1.045
spec power MCP	hp/lb/sec	260	260	193	192
spec power IRP	hp/lb/sec	301	301	214	213
spec power MRP	hp/lb/sec	320	320	218	217
spec power CRP	hp/lb/sec	332	332	221	220
MCP SLS sfc	lb/hp-hr	0.376	0.385	0.353	0.355
MCP SLS fuel flow	lb/hr	953	774	901	763
MCP SLS mass flow	lb/sec	9.74	7.73	13.23	11.20
MCP SLS gross jet thrust	lb	135	108	118	100
engine weight	lb	445	381	445	396
weight/power		0.148	0.160	0.148	0.157
P_{avail} 4k/95 MRP	hp	2168	1712	2079	1751
P_{avail} 6k/95 MRP	hp	2011	1597	1929	1625
P_{avail}/P0 4k/95 MRP		0.675	0.671	0.676	0.676
P_{avail}/P0 6k/95 MRP		0.626	0.626	0.627	0.627

Table 14. Two-pilot design excursion.

		Baseline	2 pilots	2-pilot capable
DGW	lb	9416	10113	9759
WMTO	lb	11692	12000	11835
WE	lb	6702	7097	7019
W_{rotor}	lb	759	791	775
AI	sec	1.50	1.50	1.50
tip weight	lb	13.0	13.2	13.1
solidity		2x0.061	2x0.066	2x0.063
disk loading	lb/ft^2	11.7	12.6	13.1
P takeoff	hp	2382	2463	2422
Q limit	hp	2100	2170	2134
V dash	knots	200	200	200
V max	knots	204	204	204
fuel burn	lb	812	854	832
fuel tank	lb	1096	1153	1124
cruise fuel flow	lb/hr	384	416	400
aircraft L/D_e		5.3	5.3	5.3
aircraft FM		0.63	0.64	0.63
rotor L/D_e		10.6	10.2	10.4
rotor FM		0.76	0.76	0.76
cost increment	$M	—	+0.2	+0.1

Table 15. Diameter, range, speed excursions.

		Baseline	40-ft diam.	370 km	230 knots
DGW	lb	9416	9576	10110	10751
WMTO	lb	11692	11970	11969	13438
WE	lb	6702	6902	6895	7811
W_{rotor}	lb	759	811	789	1002
AI	sec	1.50	1.50	1.50	1.5
tip weight	lb	13.0	4.9	13.1	24.7
solidity		2x0.061	2x0.040	2x0.066	2x0.070
disk loading	lb/ft^2	11.7	7.6	12.6	13.4
P takeoff	hp	2382	2403	2453	3591
Q limit	hp	2100	2119	2162	3166
V dash	knots	200	200	200	230
V max	knots	204	204	204	234
fuel burn	lb	812	782	1308	1005
fuel tank	lb	1096	1056	1766	1357
cruise fuel flow	lb/hr	384	352	408	493
aircraft L/D_e		5.3	5.8	5.3	5.0
aircraft FM		0.63	0.63	0.64	0.63
rotor L/D_e		10.6	12.2	10.3	9.9.
rotor FM		0.76	0.74	0.76	0.76
cost increment	$M	—	–0.2	+0.1	+2.0

Table 16. Six passenger design excursion.

		Baseline	6 pass.	6 pass. capable
DGW	lb	9416	10794	10054
WMTO	lb	11692	12730	12607
WE	lb	6702	7332	7235
W_{rotor}	lb	759	859	838
AI	sec	1.50	1.50	1.50
tip weight	lb	13.0	15.7	16.3
solidity		2x0.061	2x0.070	2x0.065
disk loading	lb/ft^2	11.7	13.4	12.5
P takeoff	hp	2382	2757	2744
Q limit	hp	2100	2430	2419
V dash	knots	200	200	200
V max	knots	204	205	207
fuel burn	lb	812	936	903
fuel tank	lb	1096	1263	1219
cruise fuel flow	lb/hr	384	462	430
aircraft L/D_e		5.3	5.0	5.0
aircraft FM		0.63	0.62	0.61
rotor L/D_e		10.6	9.8	10.2
rotor FM		0.76	0.77	0.76
cost increment	$M	—	+0.7	+0.6

Table 17. Disk loading sweep.

		Baseline	35-ft diam	UH60 disk loading
DGW	lb	9416	9512	9545
WMTO	lb	11692	11890	11931
WE	lb	6702	6816	6873
W_{rotor}	lb	759	774	801
AI	sec	1.50	1.50	1.50
tip wt	lb	13.0	11.0	5.1
diameter	ft	32	35	39.5
solidity		2x0.061	2x0.052	2x0.041
disk loading at DGW	lb/ft^2	11.7	9.9	7.8
disk loading at WMTO	lb/ft^2	14.5	12.4	9.73
P takeoff	hp	2382	2385	2390
Q limit	hp	2100	2102	2107
V dash	knots	200	200	200
V max	knots	204	204	204
fuel burn	lb	812	799	781
fuel tank	lb	1096	1079	1054
cruise fuel flow	lb/hr	384	371	353
aircraft L/D_e		5.3	5.5	5.7
aircraft FM		0.63	0.64	0.63
rotor L/D_e		10.6	11.2	12.1
rotor FM		0.76	0.76	0.75
cost increment	$M	—	–0.1	–0.1

Table 18. Disk loading sweep for ITEP engine, 2 pilots, 6 passengers.

		32ft diam	35ft diam	38ft diam	UH60 disk loading
DGW	lb	10329	10397	10414	10528
WMTO	lb	12911	12996	13017	13160
WE	lb	7515	7607	7646	7773
W_{rotor}	lb	803	861	909	969
AI	sec	1.50	1.50	1.50	1.50
tip wt	lb	13.4	14.7	12.9	10.6
diameter	ft	32	35	38	41.5
solidity		2x0.067	2x0.056	2x0.048	2x0.041
disk loading at DGW	lb/ft^2	12.8	10.8	9.2	7.8
disk loading at WMTO	lb/ft^2	16.1	13.5	11.5	9.73
P takeoff	hp	3000	3000	3000	3000
Q limit	hp	2412	2196	2154	2154
V dash	knots	200	200	200	200
V max	knots	208	208	208	208
fuel burn	lb	894	874	856	849
fuel tank	lb	1206	1180	1158	1146
cruise fuel flow	lb/hr	434	418	405	390
aircraft L/D_e		4.8	5.0	5.2	5.4
aircraft FM		0.62	0.62	0.63	0.62
rotor L/D_e		10.1	10.7	11.1	12.0
rotor FM		0.76	0.76	0.75	0.75
cost increment	$M	+1.0	+1.0	+1.0	+1.0

Table 19. Lift-offset compound (LOC) design excursion.

		Baseline CCH	LOC
DGW	lb	9416	10362
WMTO	lb	11692	13882
WE	lb	6702	7538
W_{rotor}	lb	759	1129
AI	sec	1.50	1.50
tip wt	lb	13.0	10.2
solidity		2x0.061	2x0.055
disk loading	lb/ft^2	11.7	12.9
P takeoff	hp	2382	2677
Q limit	hp	2100	2360
V dash	knots	200	200
V max	knots	204	204
fuel burn	lb	812	898
fuel tank	lb	1096	1214
cruise fuel flow	lb/hr	384	424
aircraft L/D_e		5.3	5.2
aircraft FM		0.63	0.71
rotor L/D_e		10.6	10.6
rotor FM		0.76	0.83
cost increment	$M	—	+0.7

Table 20. Design specifications and fallout capability.

	baseline specification	fallout capability	design excursion
mission radius	200 km	222 km (300 km at 4k/95)	370 km ΔW=700 lb
passengers	4 x 300 lb	4 x 400 lb	6 x 300 lb ΔW=600-1400 lb, ΔP=375 hp
internal payload	1200 lb	2700 lb cargo UAS (2000 lb to 600 km)	
external payload	—	3400 lb cargo UAS (2200 lb to 200 km)	
crew	1	1	2 ΔW=350-700 lb
dash speed	200 kt	Vmax 204 knots 6k/95 (218 knots 5k/ISA)	230 knots 6k/95 ΔP=1200 hp, ΔW=1335 lb
engine	scaled	—	3000 hp ΔW=250-550 lb

Figure 1. Coaxial Compound Helicopter (CCH) configuration.

	Segment	Atmosphere	Time	Distance	Speed	Engine Rating	Payload
		ft / ºF	min	km	KTAS		lb
1	taxi	4k / 95	5			100% IRP	1200
2	hover	4k / 95	2		HOGE	≤95% MRP	1200
3	climb	4k / ISA			best climb	100% IRP	1200
4	cruise	10k / ISA		150	V_{br}	≤100% MCP	1200
5	penetration	6k / 95		50	200	≤95% MCP	1200
6	hover	6k / 95	1		HOGE	≤95% MRP	1200
7	loiter	6k / 95	30		V_{be}	≤100% MCP	0
8	hover	6k / 95	1		HOGE	≤95% MRP	1200
9	penetration	6k / 95		50	200	≤95% MCP	1200
10	climb	6k / ISA			best climb	100% IRP	1200
11	cruise	10k / ISA		150	V_{br}	≤100% MCP	1200
12	hover	4k / 95	1		HOGE	≤95% MRP	1200
13	reserve	4k / 95	30 or 10%		V_{br}	≤100% MCP	1200

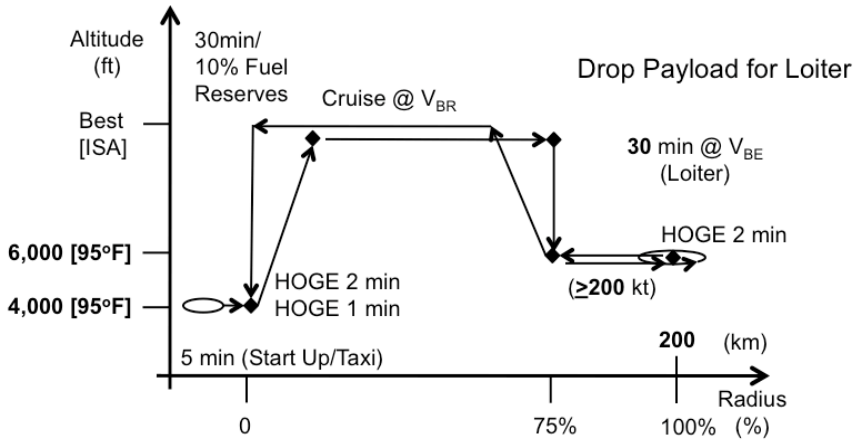

Figure 2. Design mission (urban assault) profile. Payload 1200 lb (4 passengers).

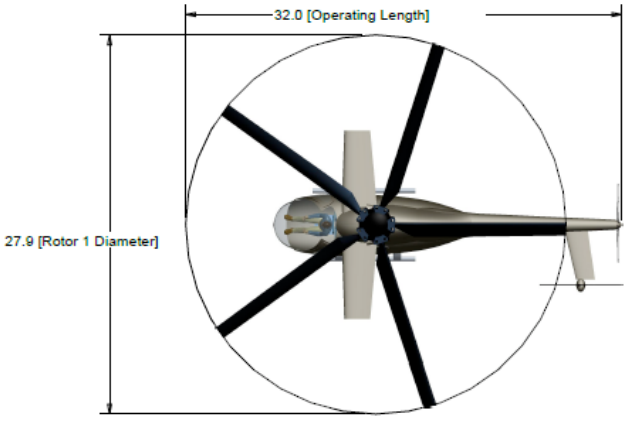

Figure 3. Small-wing compound helicopter configuration, with single main rotor (dimensions in ft).

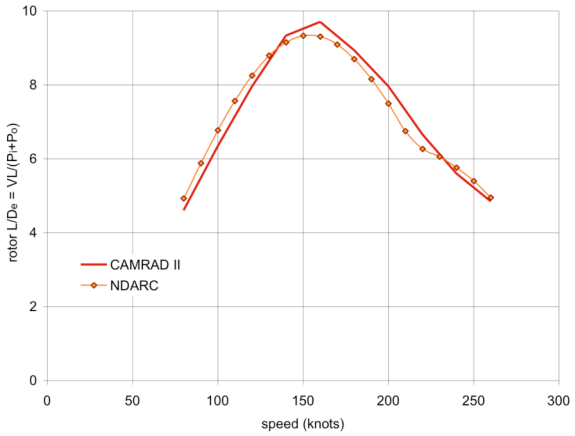

Figure 4. CAMRAD II and NDARC rotor performance for CCH coaxial rotor.

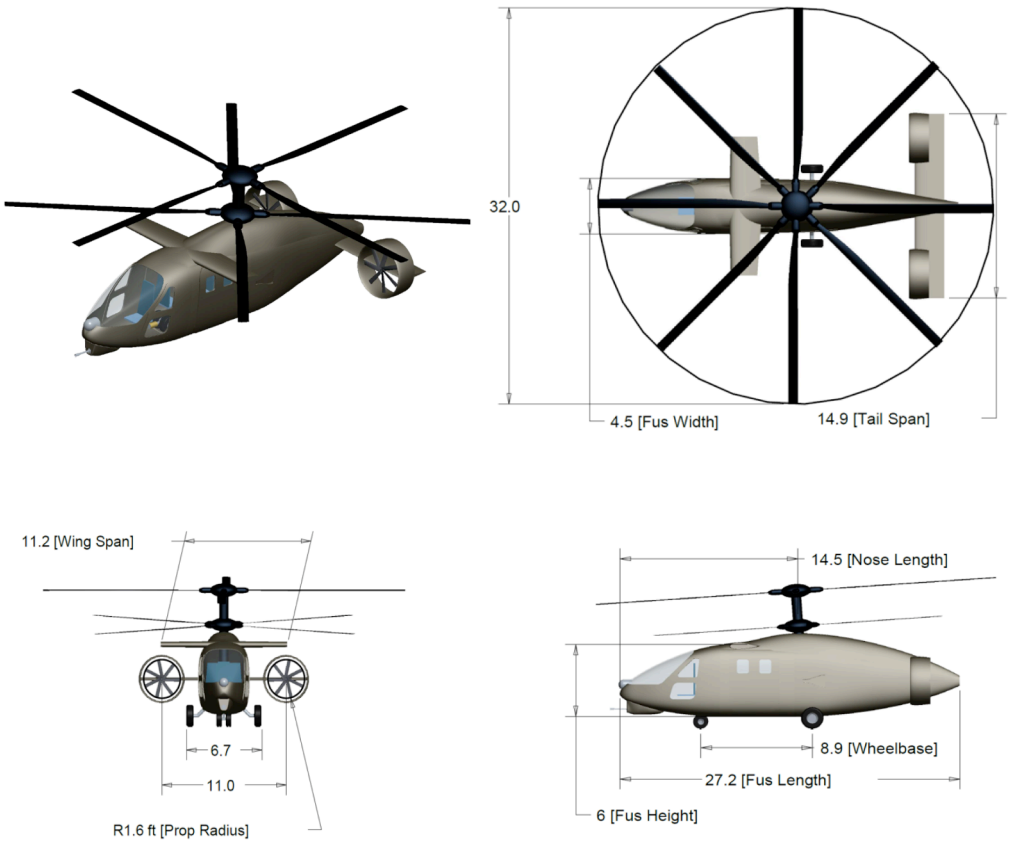

Figure 5. Baseline CCH design (dimensions in ft).

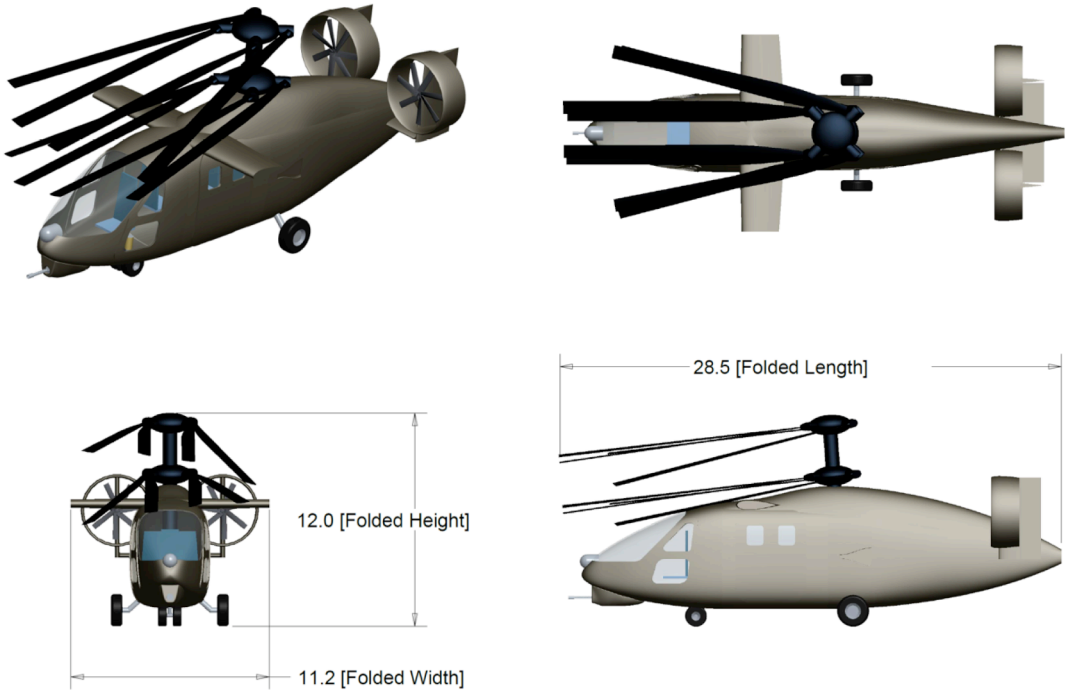

Figure 6. Baseline CCH design, folded (dimensions in ft).

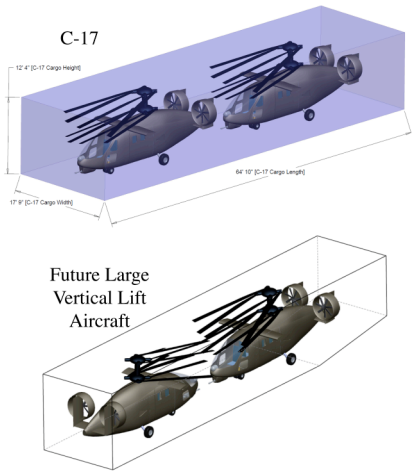

Figure 7. Baseline CCH design, transportability.

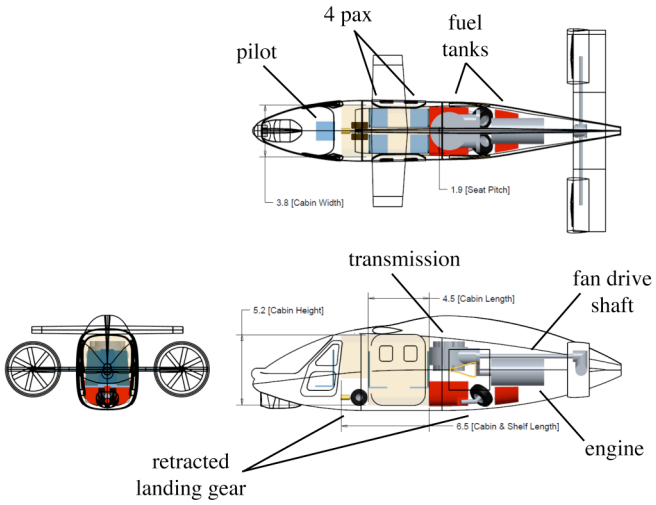

Figure 8. Baseline CCH design, inboard profile.

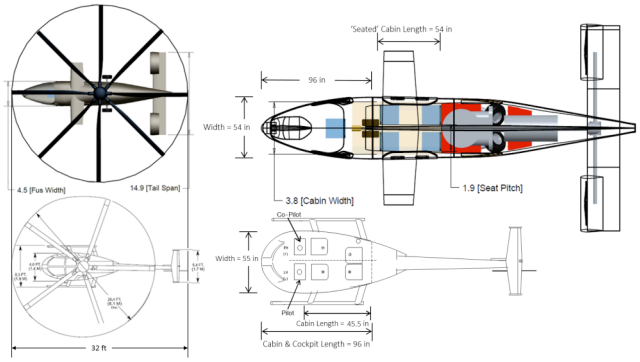

Figure 9. Comparison of operating dimensions and cabin with MD500.

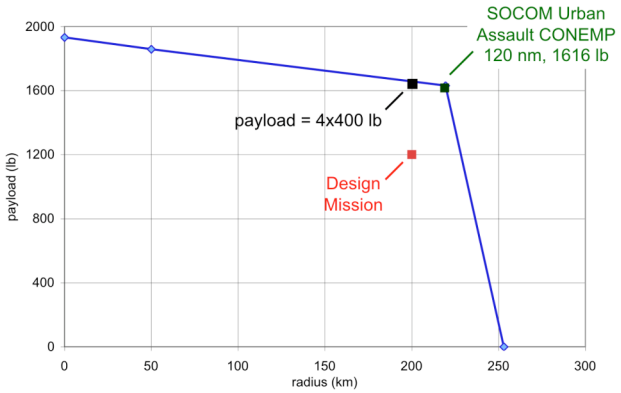

Figure 10. CCH urban assault (design mission) payload-radius.

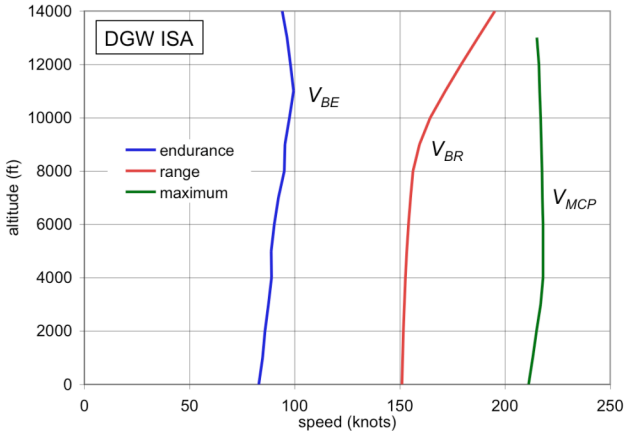

Figure 11. CCH best effort speeds as function of altitude (DGW ISA).

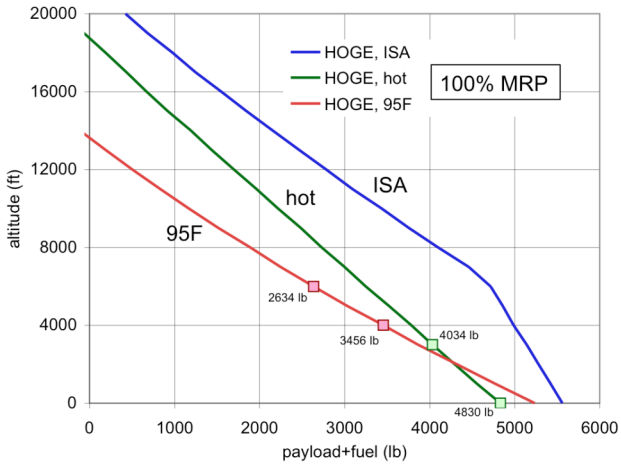

Figure 12. CCH lift capability as function of altitude altitude (HOGE at 100% MRP).

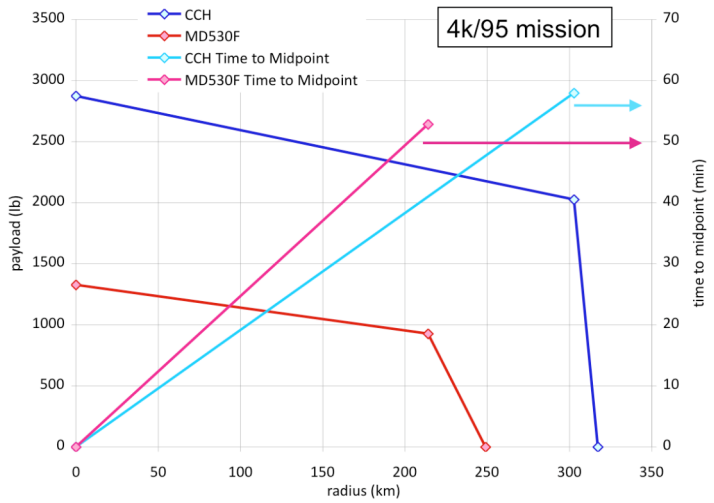

Figure 13. Comparison of CCH and MD530F payload-radius and response time.

	Segment	Atmosphere	Time	Distance	Speed	Engine Rating	Payload
		ft / ºF	min	km	KTAS		lb
1	taxi	4k / 95	5			100% IRP	1020
2	hover	4k / 95	2		HOGE	≤95% MRP	1020
3	climb	4k / ISA			best climb	100% IRP	1020
4	cruise	10k / ISA		150	V_{br}	≤100% MCP	1020
5	penetration	6k / 95		50	200	≤95% MCP	1020
6	hover	6k / 95	7.5		HOGE	≤95% MRP	1020
7	loiter	6k / 95	15		V_{be}	≤100% MCP	1020
8	hover	6k / 95	7.5		HOGE	≤95% MRP	0
9	penetration	6k / 95		50	200	≤95% MCP	0
10	climb	6k / ISA			best climb	100% IRP	0
11	cruise	10k / ISA		150	V_{br}	≤100% MCP	0
12	hover	4k / 95	1		HOGE	≤95% MRP	0
13	reserve	4k / 95	30 or 10%		V_{br}	≤100% MCP	0

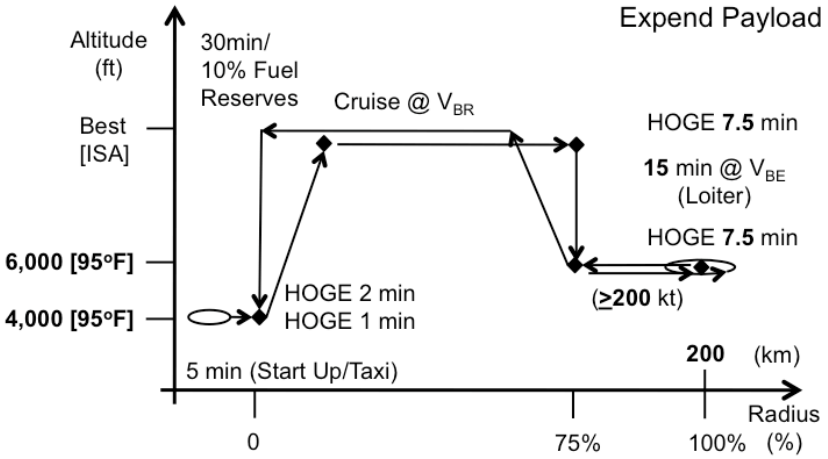

Figure 14. Light attack mission profile. Payload 1020 lb.

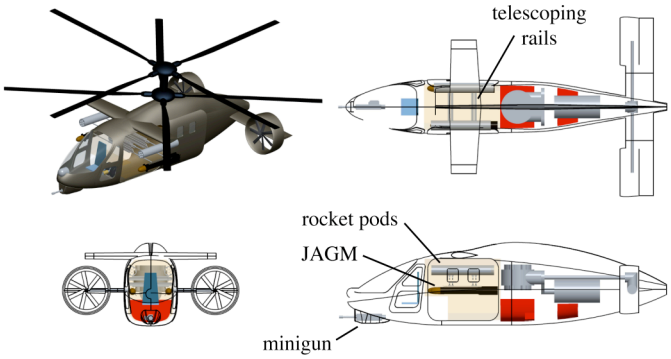

Figure 15. Light attack configuration.

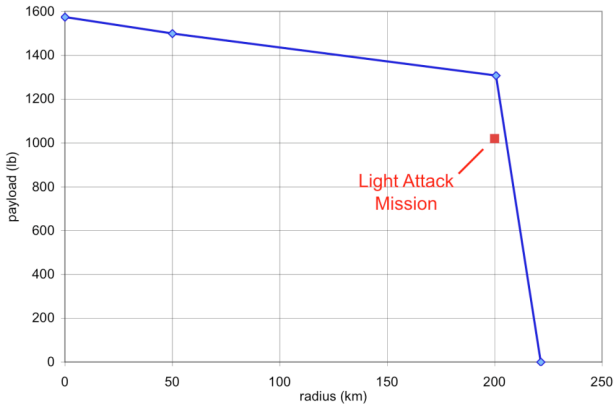

Figure 16. Light attack payload-radius.

	Segment	Atmosphere	Time	Distance	Speed	Engine Rating	Payload
		ft / ºF	min	km	KTAS		lb
1	taxi	SL / 103	5			100% IRP	1200
2	hover	SL / 103	2		HOGE	≤95% MRP	1200
3	climb	SL / ISA			best climb	100% IRP	1200
4	cruise	10k / ISA		424	V_{br}	≤100% MCP	1200
5	hover	6k / 95	1		HOGE	≤95% MRP	1200
6	idle	6k / 95	5		HOGE	100% MCP	0
7	hover	6k / 95	1		HOGE	≤95% MRP	0
8	climb	6k / ISA			best climb	100% IRP	0
9	cruise	10k / ISA		424	V_{br}	≤100% MCP	0
10	hover	SL / 103	1		HOGE	≤95% MRP	0
11	reserve	4k / 95	30 or 10%		V_{br}	≤100% MCP	0

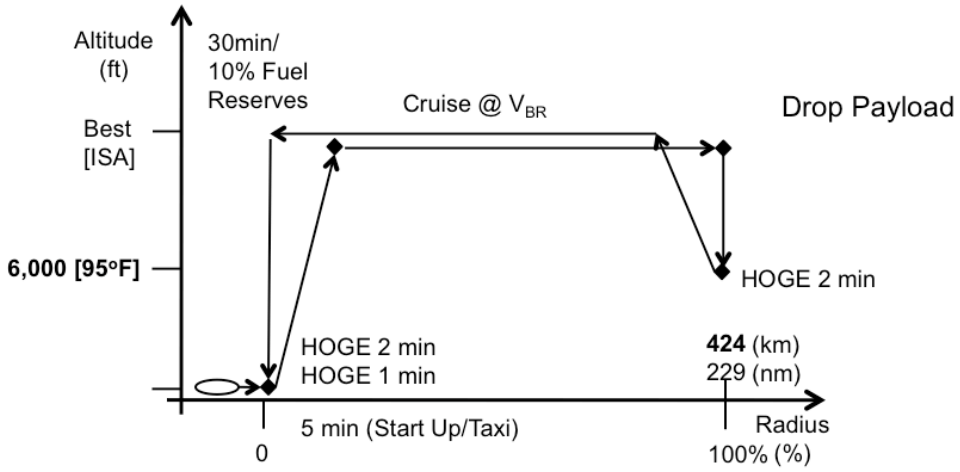

Figure 17. Cargo UAS mission profile. Payload 1200 lb.

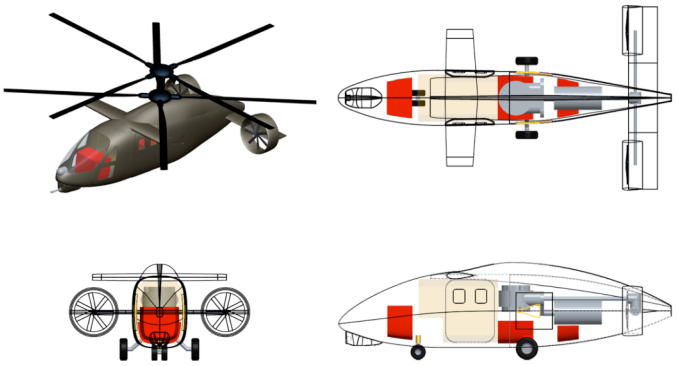

Figure 18. Cargo UAS configuration.

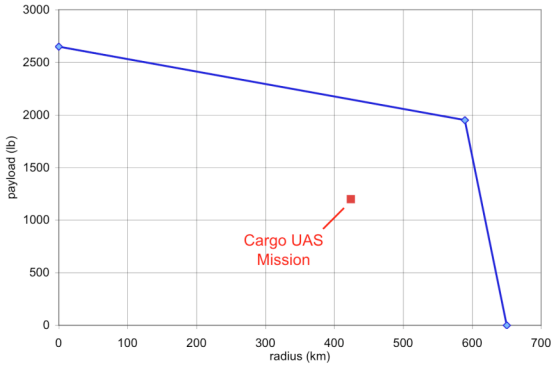

Figure 19. Cargo UAS payload-radius.

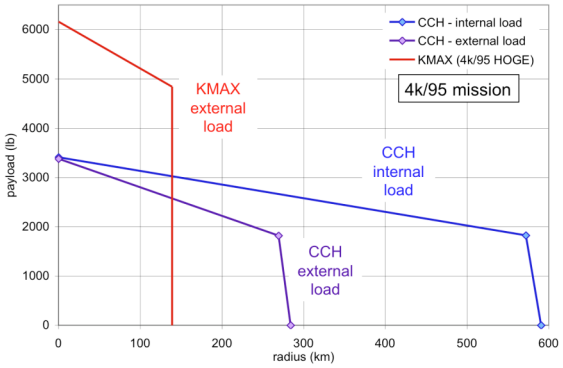

Figure 20. Comparison of CCH cargo UAS and KMAX payload-range, for external and internal load.

	Segment	Atmosphere	Time	Distance	Speed	Engine Rating	Payload
		ft / ºF	min	km	KTAS		lb
1	taxi	SL / 103	5			100% IRP	1600
2	hover	SL / 103	2		HOGE	≤95% MRP	1600
3	climb	SL / ISA			best climb	100% IRP	1600
4	cruise	10k / ISA		318	V_{br}	≤100% MCP	1600
5	penetration	6k / 95		106	200	≤95% MCP	1600
6	penetration	6k / 95		106	200	≤95% MCP	0
7	climb	6k / ISA			best climb	100% IRP	0
8	cruise	10k / ISA		318	V_{br}	≤100% MCP	0
9	hover	SL / 103	1		HOGE	≤95% MRP	0
10	reserve	4k / 95	30 or 10%		V_{br}	≤100% MCP	0

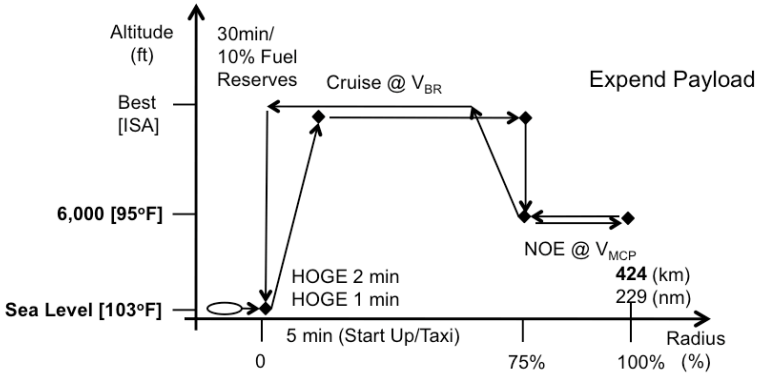

Figure 21. Counter-IADS UAS mission profile. Payload 1600 lb.

Figure 22. Counter-IADS UAS configuration.

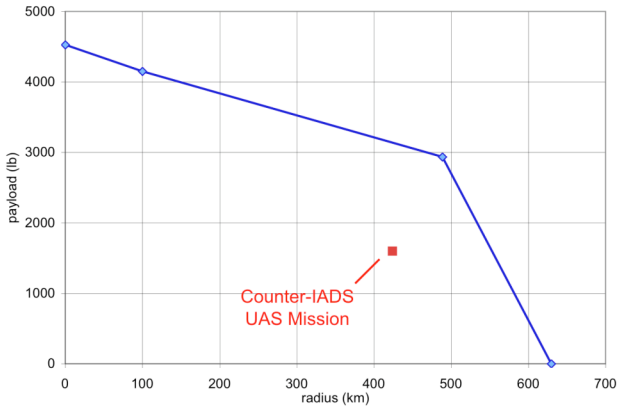

Figure 23. Counter-IADS UAS payload-radius.

	Segment	Atmosphere	Time	Distance	Speed	Engine Rating	Payload
		ft / ºF	min	km	KTAS		
1	taxi	4k / 95	5			100% IRP	625
2	hover	4k / 95	2		HOGE	≤95% MRP	625
3	climb	4k / ISA			best climb	100% IRP	625
4	cruise	10k / ISA		200	V_{MCP}	≤95% MCP	625
6	hover	6k / 95	1		HOGE	≤95% MRP	625
7	loiter	6k / 95	10		V_{bc}	≤100% MCP	960
8	hover	6k / 95	1		HOGE	≤95% MRP	960
10	climb	6k / ISA			best climb	100% IRP	960
11	cruise	10k / ISA		200	V_{MCP}	≤95% MCP	960
12	hover	4k / 95	1		HOGE	≤95% MRP	960
13	reserve	4k / 95	30 or 10%		V_{br}	≤100% MCP	960

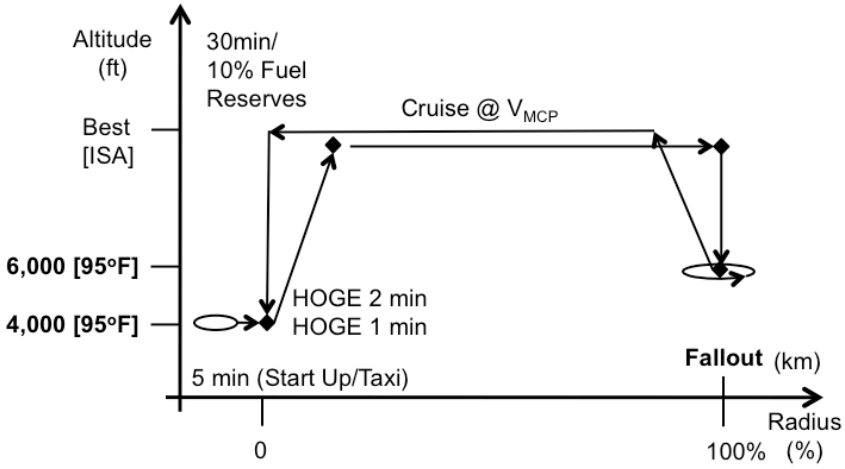

Figure 24. MEDEVAC mission profile. Payload 960 lb (single 335 lb patient).

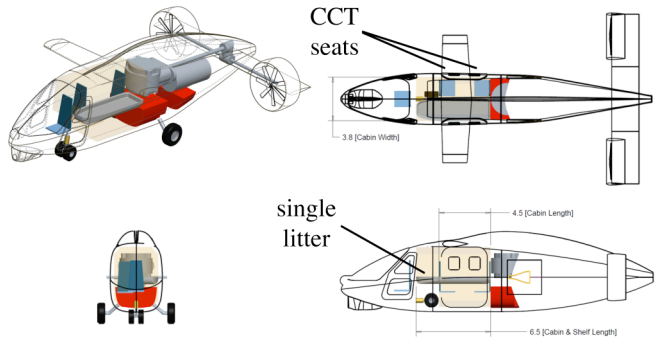

Figure 25. MEDEVAC configuration.

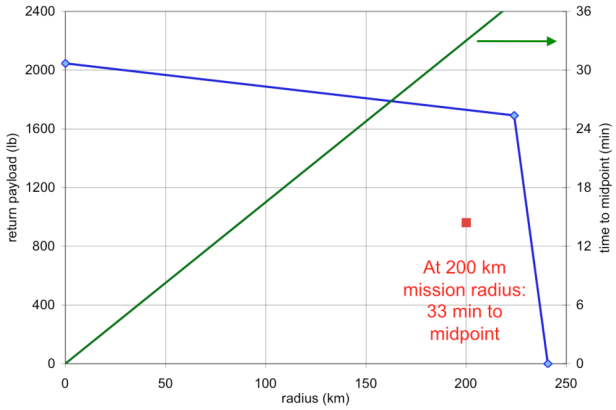

Figure 26. MEDEVAC payload-radius.

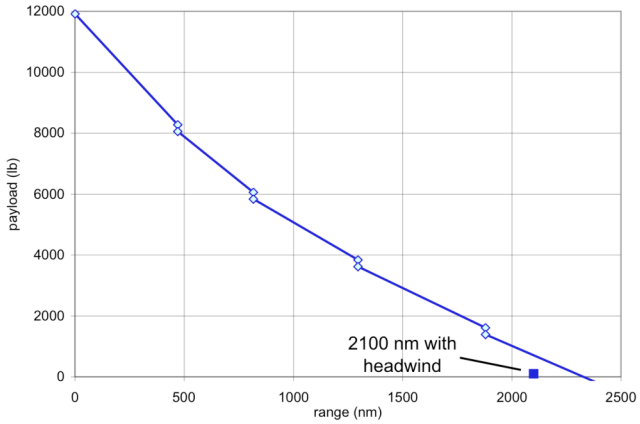

Figure 27. Self-deploy payload-range; takeoff weight 18200 lb (1.9 SDGW).

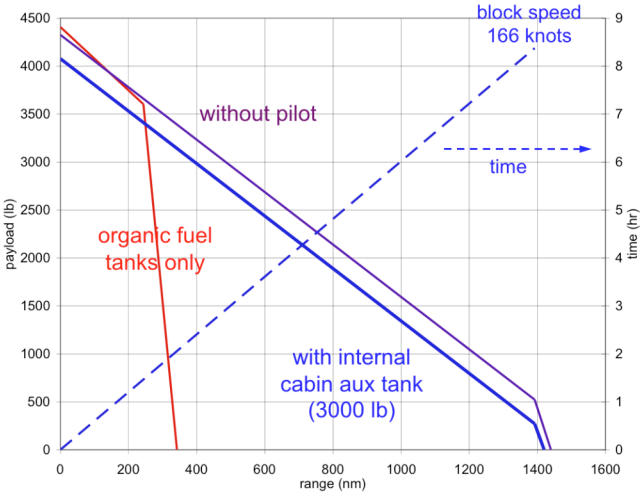

Figure 28. Deployment at best range speed.

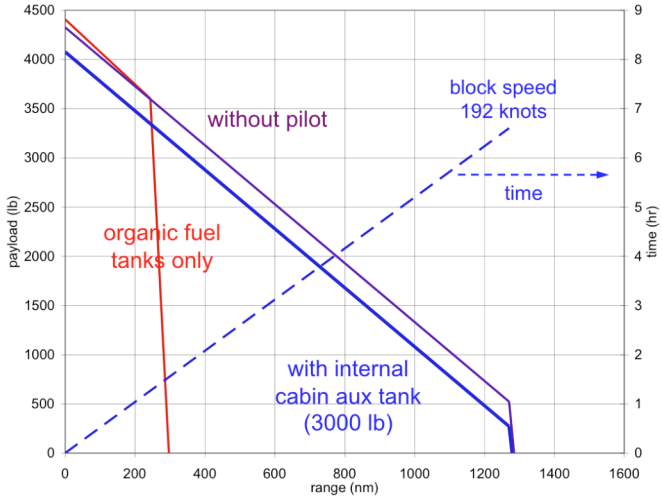

Figure 29. Deployment at maximum speed.

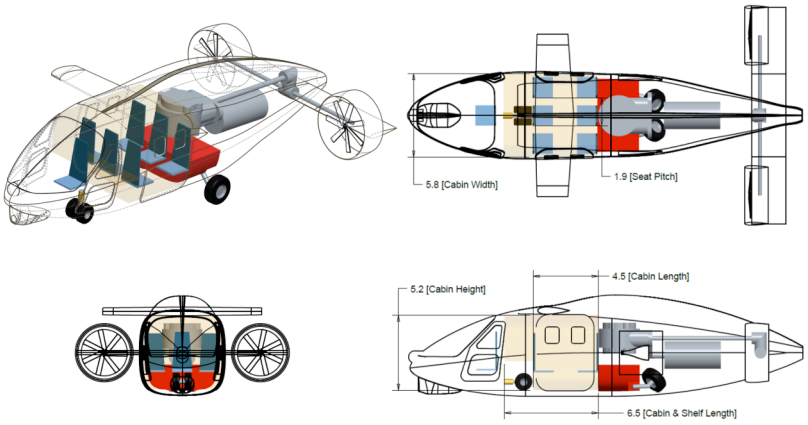

Figure 30. Six-passenger CCH configuration.

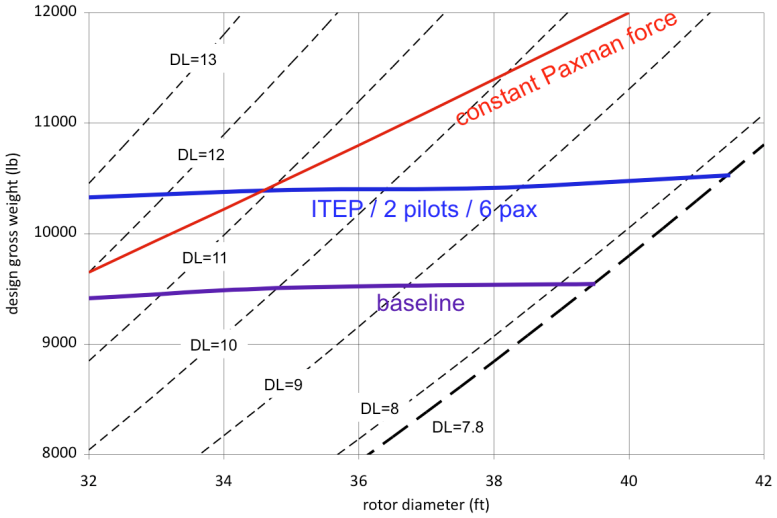

Figure 31. Aircraft size and outwash variation with disk loading. Paxman force for CCH at UH-60 value.

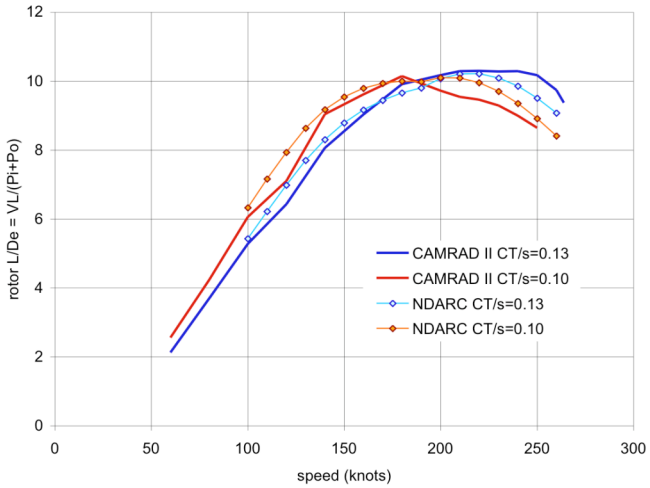

Figure 32. CAMRAD II and NDARC rotor performance for lift-offset coaxial rotor (lift offset = 0.25R).